Utrecht University

MASTER THESIS

Action potential propagation in neurons

Author
M. AMIN

Supervisor
Prof. dr. R. (René) van ROIJ

June 2019

Abstract

We study the propagation of electrical signals in neurons by numerically solving the Hodgkin & Huxley cable equations of action potential propagation for the squid giant axon. For this we represent the biological membrane as an equivalent circuit containing voltage-gated ion channels that selectively open depending on the voltage. The presence of these voltage-gated channels turn out to be critical for obtaining the standard action potential form. The results that we obtain from simulations are in good agreement with experimental recordings done by Hodgkin & Huxley. We numerically solved the Hodgkin & Huxley equations for the squid giant axon at different temperatures and studied the obtained action potentials and ionic currents as a function of time and position.

Contents

1 Introduction

The Nervous system and its regulation of bodily function and activity is a fascinating area of study. Ages of evolution have optimized our body into a machine which is able to transmit and receive information at a very rapid pace. A necessary requirement for our survival. Aside from the fact that it is fascinating to know how it works, understanding the workings of the nervous system could not only provide us with possible solutions for those that suffer from neurological disorders (a disorder of the nervous system), but it could, for instance, also lead to the development of artificial muscle fibres or even teach us ways to optimize transmission of electrical currents through conductors. So it is very relevant to study the propagation of signals through the nervous system. Questions that arise when thinking about its functions are how these signals propagate through the nervous system, what ensures their fast propagation and whether it is possible to model them by simple principles. We have set out to answer these questions by studying physical models of currents through excitable cells. An outline of this thesis will then be as follows:
First we will introduce the object of interest which is the neuron. We will briefly describe its various components and illustrate their scales by providing some experimentally measured lengths. Next we take a closer look at the membrane of our cells and introduce its various components. Having done this, we turn our attention to modelling the flow of current in excitable cells. For this, we start by representing the membrane as an equivalent circuit which we use to write down expressions for the membrane currents. Next, Using this equivalent circuit form, we derive the standard model for describing current flow in neurons called the cable model. We first look at a simple form of this cable model, in which we consider a passive membrane, and solve this to study the passive flow of current in cells. After having studied the passive flow of current in cells, we extend the model to account for the voltage dependent properties of the membrane [6]. This will lead us to the active cable model provided by Hodgkin & Huxley [6]. Finally, by solving the Hodgkin & Huxley model, we study the current flow in excitable cells and compare these results with experiments.

2 The Neuron

In Fig. 1, the structure of a neuron is represented schematically. Neurons are electrically excitable cells which are specialized in long-distance transmission of electrical signals. A neuron consists of a cell body (soma), dendrites and a single axon. Electrical impulses enter the neuron through the dendrites, into the soma and leave through the axon to excite other dendrites. The number of inputs a neuron can receive is dependent on how big its dendritic tree is. While some neurons may lack dendrites, others have a very complex dendritic tree (see Fig. 2). The axon may have branches as well, but they are not as elaborate as those made by dendrites.
The object of interest to us however, is the axon (see 3, 1). The axon is the portion of the nerve cell specialized in relaying electrical signals over long distances. Depending on the type of neuron and the size of the animal, the axon can extend from a few micrometers all the way to meters. In most animals, the axons are periodically covered by fat layers called myelin sheets (1). These myelin sheets consist of multiple layers of fat pressed on top of each other (3, [15]). The primary function of these myelin sheets is to increase the conduction velocity of signals by insulating the axon. One can compare the axon with the myelin sheets as an electric wire(axon) surrounded by insulating material (myelin). However, unlike plastic covering a typical electric wire, myelin sheets do not extend continuously along the axon, but have periodic gaps called the nodes of Ranvier (1). These gaps turn out to be the reason for the long-distance quick signal transmission. The general idea behind this faster conductive velocity is saltatory conduction [24]. However, in the following we will be working with the squid giant axon as did Hodgkin

& Huxley. The squid giant axon is an unmyelinated axon which means that we wont be delving into the precise effects of the myelin on signal propagation. Instead we will briefly come back to it after our discussion of the current flow in unmyelinated excitable cells.

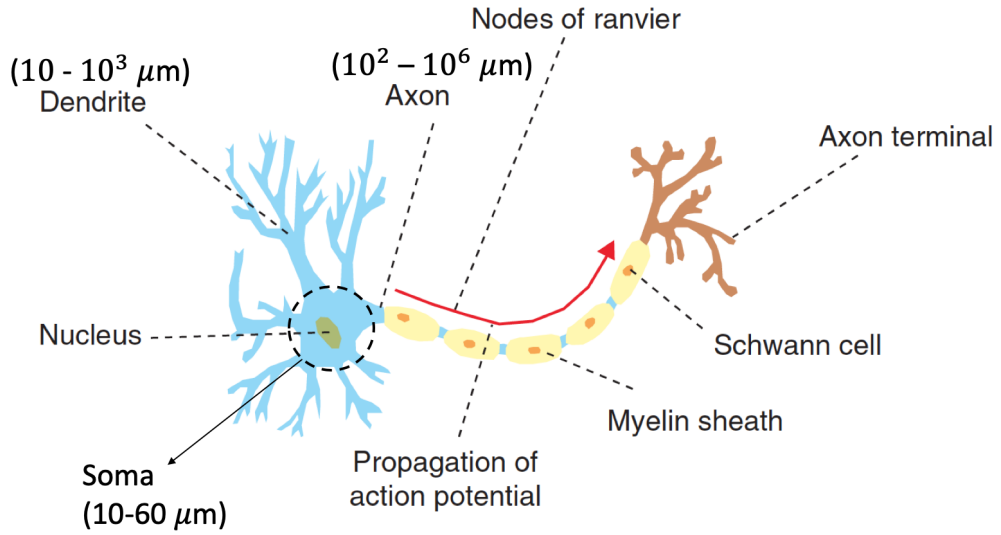

Figure 1: A schematic diagram of a neuron. The different components and some size ranges are displayed. Source(modified): [26].

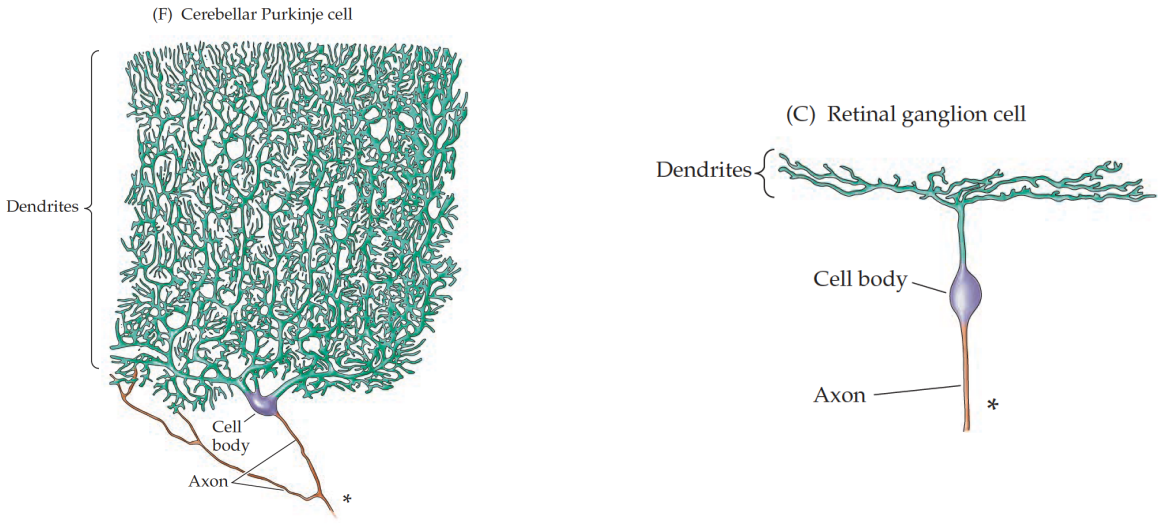

Figure 2: Neuron morphology in different human cells. The drawings are tracings of actual nerve cells stained by impregnation with silver salts. The asterisks indicate that the axon runs on much farther than shown. The drawings are not at the same scale. Source: [18].

3 The membrane

Having discussed the neuron, we now zoom in on the cell membrane. The key components of the membrane that we will be considering are shown in Fig. 4. The inside(intracellular) and outside(extracellular) solutions are separated by an insulating lipid bilayer with a thickness of approximately 5 nm. This lipid bilayer is impermeable to ions which means that there need to

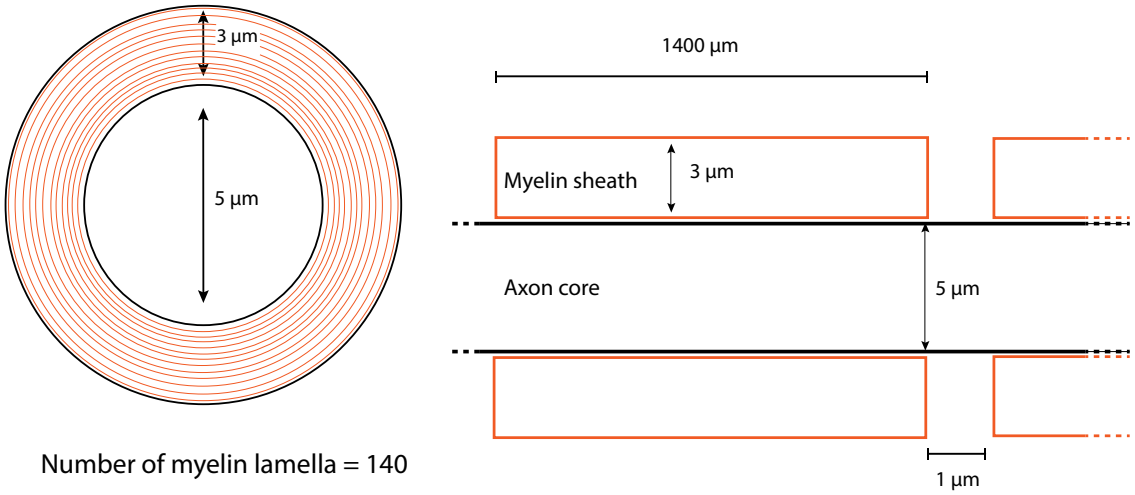

Figure 3: Schematic diagram of an axon segment of the myelinated cat nerve fibre. The values have been extracted from [11].

be other structures in the membrane that will allow ions to flow in and out of the cell. This flow is regulated by ion channels and pumps as depicted in Fig. 4.
The ion channels are protein pores in the membrane that will allow ions to enter and exit the cell. These channels can be either **passive** or **active**. The difference between these two is that active channels can close themselves depending on the value of the membrane potential, ionic concentrations or due to the presence of inactivating particles. Passive channels on the other hand have unchanged permeability and can be thought of as holes in the membrane. Both channel types exhibit **selective permeability** for certain ions. This means that they allow one particular ion to permeate the most. We label these channels by the ions to which they are most permeable. For instance, a sodium(Na^+) channel will allow mostly sodium ions to enter and leave the cell. In Fig. 4, both a sodium as well as a potassium channel is illustrated.
Finally, the membrane also contains various ion-pumps(ion-exchangers). These are protein structures in the membrane that actively pump certain ions in and out of the cell. If left to their own devices, ions will flow from large to low ion concentrations such that the concentration gradient is lowered. The ion pumps however, counteract this flow by pumping in the oppostite direction. There are many pumps of which one is illustrated in Fig. 4. This sodium-potassium exchanger pumps 2 K^+-ions in and 3 Na^+-ions out of the cell. The energy required for this process is provided by the cell metabolism. Since this sodium-potassium pump pushes 2 potassium ions in and 3 sodium ions out of the cell, there is a net loss of charge in the cell. These types of pumps we call **electrogenic**. There are also non-electrogenic pumps such as the sodium-hydrogen pump which pushes one H^+-ion out of the cell against its concentration gradient and one Na^+-ion into the cell. With this exchange, the Na^+-ions flow down their concentration gradient which will supply the energy for the flow of H^+-ions out of the cell. Hence the cell does not need to provide any energy for this exchange.
These pumps make it possible for the cell to maintain a true steady state at rest. However, we are interested in studying action potentials, which are fast disturbances to the steady state, and

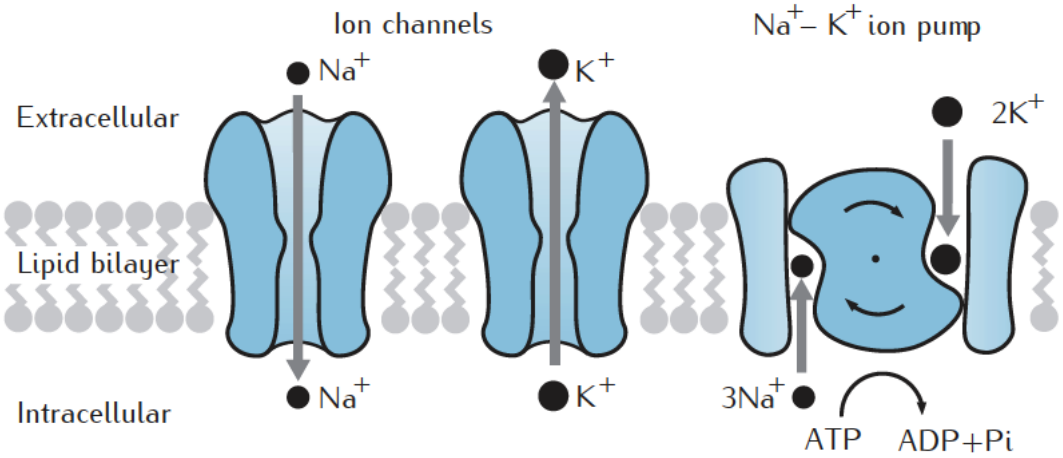

Figure 4: Components of the membrane. The inside and outside solutions are separated by a lipid bilayer which is impermeable to ions. The ion channels are clusters of protein that allow certain ions to pass. Finally, the $Na^+ - K^+$ pump is displayed which exchanges three Na^+ ions from the inside with two K^+ ions from the outside using the energy from the hydrolysis of ATP. Source: [23].

it turns out that the immediate effects of shutting down these pumps is small [16]. Furthermore, a nerve cell can transmit hundreds of action potentials after its ion pumps have been shut down [16]. Hence, from now on we will consider a simplified membrane where we ignore the ion-pumps.

3.1 Equilibrium potentials

Having looked at the membrane and its key components, we now turn to the membrane potentials, and in particular the resting membrane potential. All electrical signals of the nervous system are caused by membrane potentials (which by standard convention is defined as the intracellular minus the extracellular potential) due to the flow of ions through ion channels. In our study of the propagation of these membrane potentials along the axon, a key element that we need to understand first is the resting membrane potential. Before we can talk about the resting potential of the membrane however, we first need to consider when the flow of a particular ion through its channel reaches equilibrium. The hope is that if we can determine the equilibrium potentials for all permeable ions, we can combine these to determine the full resting potential of the membrane.
In order to accomplish this, we first need to explain what we mean by an equilibrium potential for a permeable ion. Hence, consider the example given in Fig. 5. We start with two solutions, consisting of K^+ cations and arbitrary anions A^-, of different concentrations separated by a semi-permeable membrane that only allows potassium ions to pass (5a). Initially, both solutions are charge neutral. Because the concentration of K^+ ions is bigger in the left solution compared to the right, there will be a net potassium flux to the right. Since the anions cannot pass the membrane, a net charge will set on both ends of the membrane. The left solution lost cations and hence will acquire a net negative charge while the right solution gained cations and hence will gain a net positive charge. Note that these charges are confined to the membrane surface as an electrical double layer [16]. These net charges then cause an electrical force which results in a potassium current to the left that counteracts the diffusion current (5b). After some time, the electric forces have grown large enough to fully counter the thermal forces. At this point, there is no net current present and the system is said to be in equilibrium. The potential

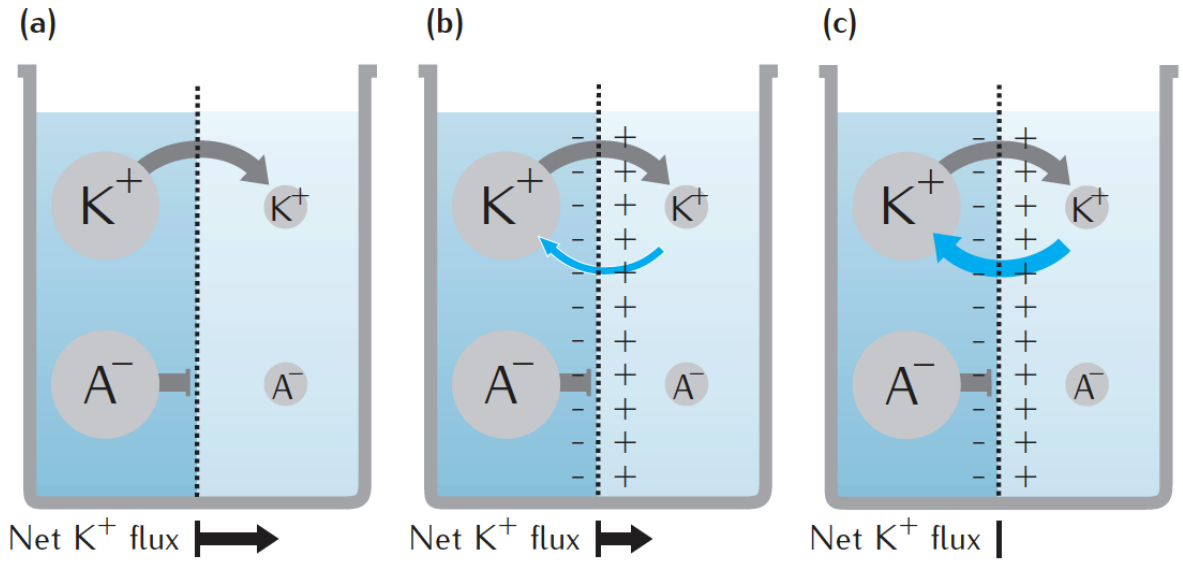

Figure 5: Visualization of the potassium currents through K^+ channels due to thermal and electrical forces. a) Because of the concentration gradient, there will be a net K^+ flux to the right. b) electrical forces give rise to a potassium current to the left. c) The thermal and electrical forces have balanced each other out. The system has reached equilibrium. Source: [23].

difference at which the system is at equilibrium is called the equilibrium potential for that ion. For the particular example of Fig. 5, we considered K^+ ions, but the same could be done for the other permeable ions.
One can determine the equilibrium(Nernst) potentials for these ions by equating the intracellular and extracellular chemical potentials. These are given by:

$$\begin{aligned} E_K &= \frac{k_B T}{e} \ln \frac{c_{K,o}}{c_{K,i}} \\ E_{Na} &= \frac{k_B T}{e} \ln \frac{c_{Na,o}}{c_{Na,i}} \end{aligned} \tag{1}$$

Where k_B is the Boltzmann constant, T is the absolute temperature, e is the elementary charge and c_o/c_i is the ratio of the outside and inside concentrations of ion X. In table 1 the concentrations and corresponding Nernst potentials for K^+ and Na^+ are given for a squid giant axon at a temperature of 23°C. Note that the initial and final concentrations of the ions will differ due to the ionic currents. However, as it turns out, this change is very minimal. In fact, the amount of ions on the membrane is millions of times smaller than the amount in the cytoplasm [23] which means that we can simplify our problem by considering the ion concentrations to be constant.

Ion	*Internal concentration (mmol/L)*	*External concentration (mmol/L)*	*Nernst potential (mV)*
$[Na^+]$	50	460	57
$[K^+]$	400	20	–77

Table 1: Ion concentrations measured for the squid giant axon at a temperature of 23°C. Source: [26]

Having discussed the equilibrium potentials of ions, one is tempted to think that the resting

potential of the membrane is just the sum of the Nernst potentials. This is however not quite correct. In fact, in what follows, we will show that Nernst potentials need to be weighted by the different conductivities of the membrane for different ions.

3.2 Equivalent circuit

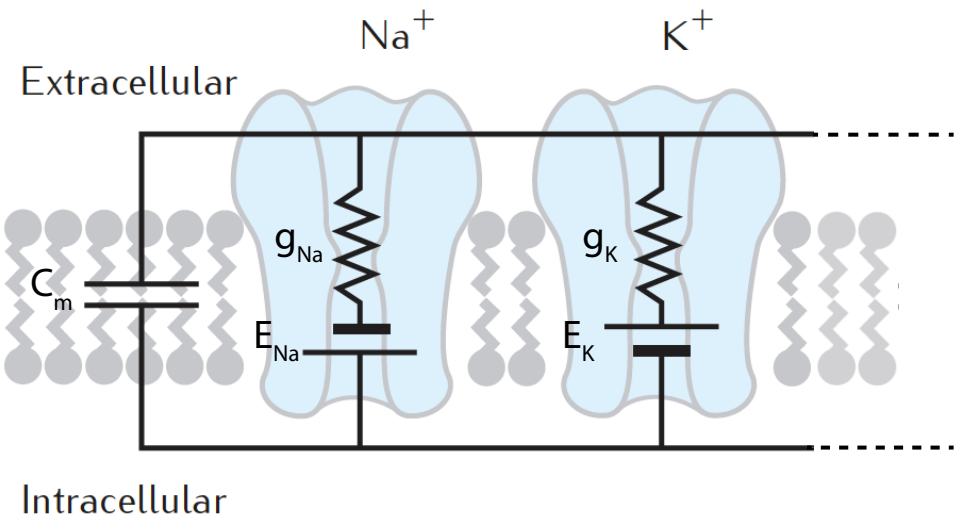

Figure 6: The equivalent electrical circuit of a patch of membrane that contains sodium (Na) and potassium (K) ion channels in parallel with a capacitance C_m. Source: [23](modified).

When considering the example above, we found out that the membrane can both separate charges as well as conduct electric currents which is carried by ions. These are properties which resemble those of an electrical circuit. Hence we would like to represent the membrane as a combination of electrical circuit components. The fact that it can separate charge, means that one of these components must be a capacitor. Next we consider the conduction of ionic currents. Many different models have been devised to describe the ionic currents, but the one which we will be using is the Ohm's law description used by Hodgkin and Huxley in their work on nerve excitation [6]. In this description, the ionic currents through K^+ and Na^+ channels are given by:

$$\begin{aligned} I_K &= g_K(V_m - E_K) \\ I_{Na} &= g_{Na}(V_m - E_{Na}) \end{aligned} \tag{2}$$

Where V_m is the membrane potential and g_K, g_{Na} are the potassium and sodium ion channel conductivity's. One important thing to note here is that in excitable cells, these conductivity's are in fact functions of voltage and time and not constants. We will look at the full form of these conductivity's later but for now we do not need to know them. So we can represent the ion channels by resistors, corresponding to the respective conductances g_K, g_{Na}, in series with electrochemical batteries that are given by the Nernst potentials E_K, E_{Na}. With this we have represented the membrane components as electrical components which, when put together, yield us the **equivalent circuit** illustrated in Fig. 6. Note that the poles of the batteries match the convention we use for the membrane potential (inside minus outside potential). A positive

Nernst potential means that the lower wire is at a higher potential and hence this is where the plus pole lies. Similarly, a negative Nernst potential means that the plus pole is connected to the upper wire.
Now that we have managed to represent the membrane as an equivalent electrical circuit, we turn to the resting membrane potential. The potential across the membrane given by V_m leads to a capacitive current $C_m dV_m/dt$, and ionic currents I_K, I_{Na}. Then by Kirchoff, we require that the sum of all currents in a closed circuit be zero. Which gives us the equation:

$$C_m \frac{dV_m}{dt} = -I_{Na} - I_K = -g_{Na}(V_m - E_{Na}) - g_K(V_m - E_K). \tag{3}$$

In the resting state, where $V_m = E_r$, the membrane potential is independent of time which means that

$$\frac{dV_m}{dt} = 0 \tag{4}$$

Plugging this into the equation above yields us the following expression for the resting potential E_r:

$$-g_{Na}(E_r - E_{Na}) - g_K(E_r - E_K) = 0 \tag{5}$$

Rewriting this, we arrive at the expression for the resting membrane potential:

$$E_r = \frac{g_{Na}E_{Na} + g_K E_K}{g_{Na} + g_K} \tag{6}$$

Hence we see that indeed the resting potential is not just the sum of the equilibrium potentials. Instead, the equilibrium potentials are weighted by their respective conductances and normalized by the sum of the conductances.

4 The passive cable model

Symbols:

i_{m}	Outward membrane current per unit length [μA/cm]
i_{ax}	Longitudinal current through the axon core [μA]
V_{ax}	Potential inside the axon core [mV]
V_{o}	Extracellular potential [mV]
$V_m = V_{\mathrm{ax}} - V_{\mathrm{o}}$	Membrane potential [mV]
$V = V_m - E_r$	Departure of V_m from its resting value [mV]
E_r	Rest value of V [mV]
r_{ax}	Axon core resistance per unit length [kΩ/cm]
R_{ax}	Axon core resistivity [kΩ cm]
r_{m}	Membrane resistance for unit length [kΩ cm]
R_{m}	Resistance across a unit area of membrane [kΩ cm^2]
c_{m}	Membrane capacitance per unit length [μF/cm]
C_{m}	Membrane capacitance per unit area [μF/cm^2]
$\lambda = (r_m/r_{ax})^{1/2}$	Length constant of core conductor [cm]
$\tau = r_m c_m$	Passive membrane time constant [ms]
d	Axon core diameter [cm]

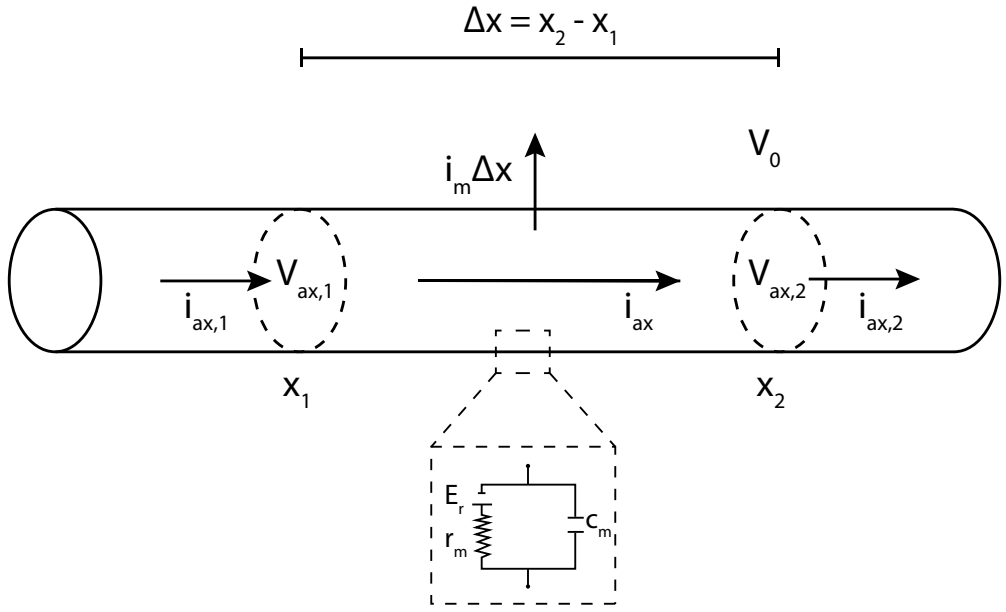

Figure 7: Longitudinal and membrane currents for a segment Δx of the passive axon. Here E_r is the resting potential of the membrane.

In the previous sections, we looked at the membrane and its components. We defined the membrane potential as being the difference between the intracellular and extracellular potentials and studied the resting potential of the membrane. First we defined the equilibrium potentials of each ion and moved on to represented the membrane as an equivalent electrical circuit consisting of a capacitance(representing the lipid-bilayer) in parallel with conductances(representing the ion channels). We found out that the resting potential is not just the sum of the equilibrium potentials, but is instead weighted by the conductances.
Until now, we have been considering the currents that can leave the axon through the membrane. Now we would like to add the longitudinal currents through the axon core into the equations. For this we will introduce a cable theory for the axon that will complete our equivalent electrical circuit (see Fig. 7 & 8). We start with the simple case of a passive membrane. That is, a membrane with a leak channel given by a constant resistance. One can imagine these channels as pores through which currents can escape the axon core when the membrane is not at rest. By using some basic laws such as Kirchhoff and Ohm's law, one can show that in the cable model, the membrane potential $V(x,t)$ at position x and time t is given by the second order equation:

$$\lambda^2 \frac{\partial^2 V}{\partial x^2} = \tau \frac{\partial V}{\partial t} + V. \tag{7}$$

Where λ and τ are the length and time constants which are material dependent. In the following, we will derive the above equation and look at some numerical solutions.

4.1 Cable model assumptions & derivation

- The first assumption we make is that the potential $V = V(x,t)$ is only dependent on the distance in the axon core, denoted by x. We neglect radial and angular dependences.

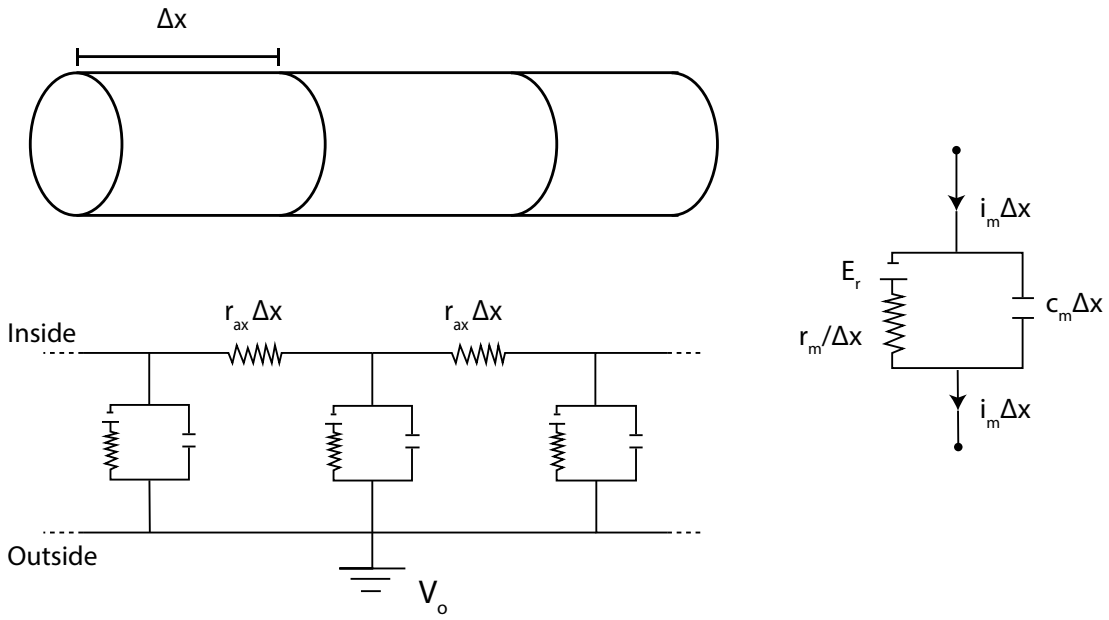

Figure 8: A compartmental model of the passive axon with r_{ax} and r_m the longitudinal resistance per unit length and membrane resistance for unit length respectively.

- The second assumption is that the intracellular medium is a simple ohmic resistance [19]. In other words, we can describe the resistance in the core by the resistance per unit length r_{ax} [Ω/cm].
- Now we apply Ohm's law to the cylindrical geometry. By taking Δx to be very small we can assume that i_{ax} [A] is constant along the increment. Then by ohm's law we have the relation

$$\Delta V_{ax} = -i_{ax} r_{ax} \Delta x \tag{8}$$

  Here the minus signs ensures that when i_{ax} is positive (positive charge moves in the direction of increasing x), $V_{ax,1} > V_{ax,2}$ since then position 1 will be more positive compared to position 2. Now we can divide each side by Δx and take the limit $\Delta x \to 0$ to obtain:

$$\frac{\partial V_{ax}}{\partial x} = -i_{ax} r_{ax} \tag{9}$$

- Next we apply conservation of current. This tells us that if $\Delta i_{ax} \neq 0$, the excess current must leak out of the membrane as i_m (see Fig. 7 & 8). Again by taking the increment to be small such that the currents don't change, we have that the total amount of membrane current is equal to $i_m \Delta x$. Then current conservation implies:

$$i_m \Delta x = -\Delta i_{ax} \tag{10}$$

  Again we divide both sides by Δx and take the limit $\Delta x \to 0$ to obtain:

$$i_m = -\frac{\partial i_{ax}}{\partial x} \tag{11}$$

- Now we can combine eq's 8 & 11 to obtain:

$$\frac{\partial^2 V_{ax}}{\partial x^2} = i_m r_{ax} \tag{12}$$

- In many cases of interest the external potential V_o has very small variation w.r.t x compared to the inside potential V_{ax} [19]. Hence we have $\partial V_o / \partial x = 0$.

- The membrane potential difference is defined as $V_m = V_{ax} - V_o$. Furthermore, we define the departure of V_m from its resting value as $V = V_m - E_r$. Here E_r is the resting potential of the membrane. This resting potential is set up by the selective diffusion of ions between the cytoplasm and the extracellular solution. Combining these two relations give us:

$$V = V_{ax} - V_o - E_r. \tag{13}$$

  For a uniform membrane we must have $\partial E_r / \partial x = 0$. Together with $\partial V_o / \partial x = 0$ we can differentiate (13) to obtain:

$$\frac{\partial^2 V}{\partial x^2} = \frac{\partial^2 V_{ax}}{\partial x^2} \tag{14}$$

  Using this and equation 12 we get:

$$\frac{1}{r_{ax}} \frac{\partial^2 V}{\partial x^2} = i_m \tag{15}$$

- Now we finalize the derivation of the simplest model by assuming a **passive membrane** (see Fig. 8). In the passive membrane model we assume constant trans-membrane resistance and emf. The standard electrical circuit representation of a passive membrane consists of a capacitor (representing the lipid bi-layer) electrically in parallel with a battery where the emf equals the resting potential of the membrane.

  The total outward membrane current $i_m \Delta x$, is the sum of the resistive and capacitive current given by:

$$i_m \Delta x = (V_m - E_r)(\frac{\Delta x}{r_m}) + (c_m \Delta x)(\frac{\partial V_m}{\partial t}) \tag{16}$$

  Now we can simplify this by dividing by Δx, using $V = V_m - E_r$ and that E_r is independent of time to obtain:

$$i_m = \frac{V}{r_m} + c_m \frac{\partial V}{\partial t} \tag{17}$$

- Finally we can equate (15) and (17) to obtain the passive membrane cable equation

$$\frac{r_m}{r_{ax}} \frac{\partial^2 V}{\partial x^2} = r_m c_m \frac{\partial V}{\partial t} + V \tag{18}$$

  Here we can define the time and length constants $\tau = r_m c_m$ and $\lambda^2 = \frac{r_m}{r_{ax}}$ respectively, to obtain eq (7):

$$\lambda^2 \frac{\partial^2 V}{\partial x^2} = \tau \frac{\partial V}{\partial t} + V \tag{19}$$

Parameter	Symbol	Units	Squid[1]	Lobster[2]	Crab[3]	Lobster[4]	Earthworm[5]	Marine worm[6]
Axon diameter	d	μm	500	75	30	100	105	560
Length constant, with $r_e = 0$	λ	cm	0.65	0.25	0.23	0.51	0.4	0.54
Input resistance, for x to $\pm\infty$, with $r_e = 0$	$R_{\pm\infty}$	Ω	5×10^3	1.8×10^5	1.5×10^6	2.5×10^5	4.6×10^5	6.2×10^4
Core resistance, per unit length	r_i	Ω/cm	15×10^3	1.4×10^6	13×10^6	1×10^6	2.3×10^6	23×10^4
Membrane resistance, for unit length	r_m	Ω cm	6.5×10^3	9×10^4	0.7×10^6	0.23×10^6	0.37×10^6	6.8×10^3
Intracellular resistivity	R_i	Ω cm	30	60	90	80	200	57
Membrane resistivity	R_m	Ω cm^2	1×10^3	2×10^3	7×10^3	8×10^3	12×10^3	1.2×10^4
Membrane time constant	τ	ms	1	2	7		3.6	0.9
Membrane capacitance	C_m	μF/cm^2	1	1	1		0.3	0.75

Figure 9: Cable parameters for invertebrate giant axons. Source: [19]

4.2 Physical meaning of time/length constant

4.2.1 time constant τ

Following excitation, the membrane potential has a decay for which the time course is given by $\tau = r_m c_m\ [s]$. The fact that τ is a measure for the decay of the membrane potential can be shown easily for a spatially uniform membrane potential ($V(x,t) = V(t)$) for which eq (7) reduces to

$$\frac{dV}{dt} = -\frac{1}{\tau}V \tag{20}$$

Which has the general solution

$$V(t) = V_0 \exp(-t/\tau) \tag{21}$$

Where $V(0) = V_0$. From the equation above it is clear that τ is the decay constant.
When the membrane potential is not spatially uniform however, its passive decay is more complicated than the result given above.

4.2.2 length constant λ

λ is a characteristic length scale of the nerve cylinder which is a measure for how far a potential will travel along the axon via passive conduction. In order to see this, we consider the steady state where V depends on the position but not time. Hence, we have that $\partial V/\partial t = 0$ and equation (7) reduces to:

$$\lambda^2 \frac{d^2V}{dx^2} = V \tag{22}$$

Now consider a semi-infinite cylinder starting at $x = 0$ and extending to $x = \infty$. Then the general solution is given by:

$$V(x) = V_0 \exp(-\frac{1}{\lambda}x) \tag{23}$$

Where $V(0) = V_0$. From this solution it is clear to see why λ is a natural length scale for the nerve cylinder. As you progress further away from $x = 0$, the potential decreases with a decay constant given by λ. When you reach $x = \lambda$, the potential has decreased to $1/e$ of V_0.
In Fig. 9 a collection of length and time constants are displayed for invertebrates that possess large axons.

5 Numerical solution of the passive cable equation for the squid giant axon

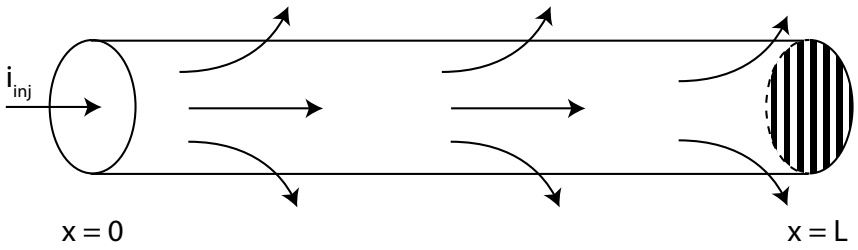

Figure 10: Passive cable with sealed ends where we inject a current i_{inj} at $x = 0$ for a certain amount of time.

Now we turn to numerically solving the passive cable equation (7) and studying its results. In section 9, we discretize the passive cable equation and show how to incorporate relevant boundary conditions. In this section we will present the results that we obtained by solving the set of discretized equations of section 9.
Consider the initial value problem displayed in Fig. 10. The boundary conditions are given by eq (69). We start with an axon that is initially at rest everywhere. Then, Starting at $t = 0$, we inject 10 μA of longitudinal current at position $x = 0$ for a total time of 7 ms before we seal this end. Using this initial state and the sealed end boundary conditions, we then solve for the membrane potential as a function of time and space.
The parameters that we used for our simulations are those for the squid giant axon as shown in table 9. These are:

$$\begin{aligned} d &= 500\ \mu\text{m}, \\ R_{ax} &= 30\ \Omega\text{cm}, \\ R_m &= 1000\ \Omega\text{cm}^2, \\ C_m &= 1\ \mu F/\text{cm}^2, \\ \lambda &= 0.65\ \text{cm}, \\ \tau &= 1\ \text{ms}. \end{aligned} \tag{24}$$

Furthermore, we choose our axon dimensions to be:

$$\begin{aligned} L &= 50\ \lambda, \\ T &= 50\ \tau, \\ N_x &= 1000, \\ N_t &= 1000. \end{aligned} \tag{25}$$

The results that we obtained are shown in Fig. 11.
By looking at these results, we observe that we can divide the course of the membrane potentials into three parts.

- The first part is the **charging of the capacitances**. In this phase which takes a little over 2τ ms, the capacitances will be charged to their maximum values.
- After the capacitances are fully charged, we enter the **steady state** phase in which the potentials are no longer dependent on time. We have shown previously that in this state, the potentials decay exponentially w.r.t the space variable x given by the length constant λ: $V(x) = V_0 \exp(-x/\lambda)$.
- The final phase is the **discharging** phase in which we stop injecting current and the potentials rapidly decay back to the rest potential. Note that the positions a bit further away from the injection site decay slower since there will still be some left-over longitudinal current that enters these parts.

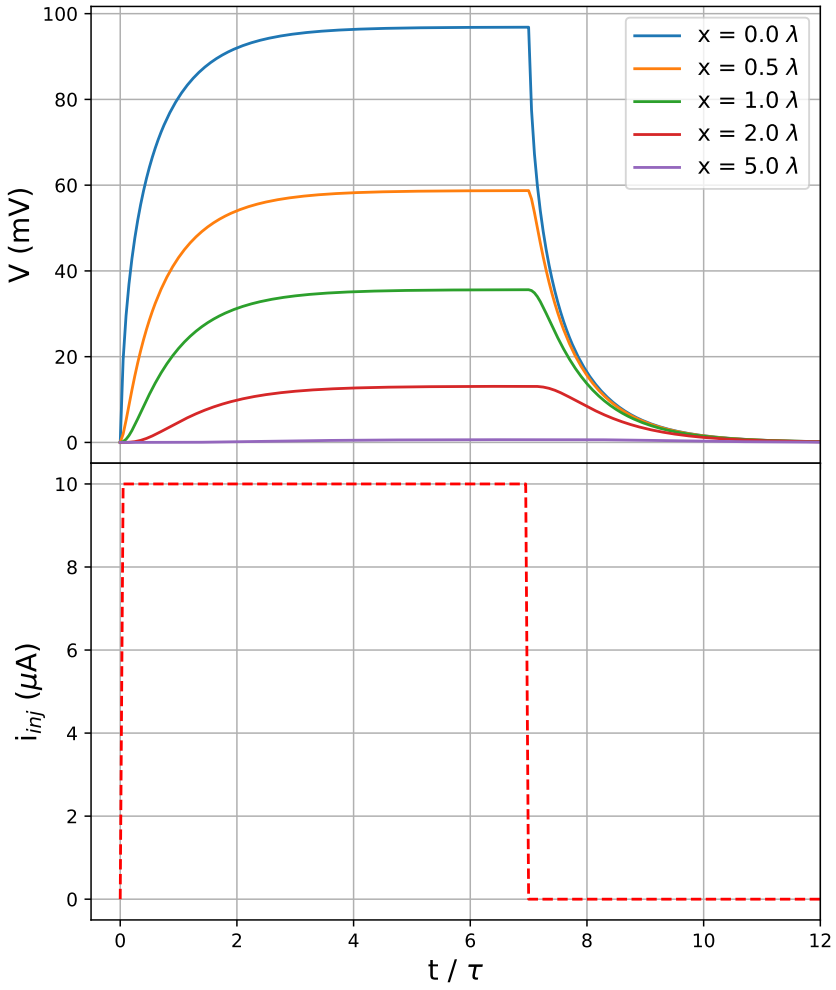

Figure 11: Solution of the passive cable equation (7) for the squid giant axon. The membrane potential is plotted as a function of time at various spatial positions.

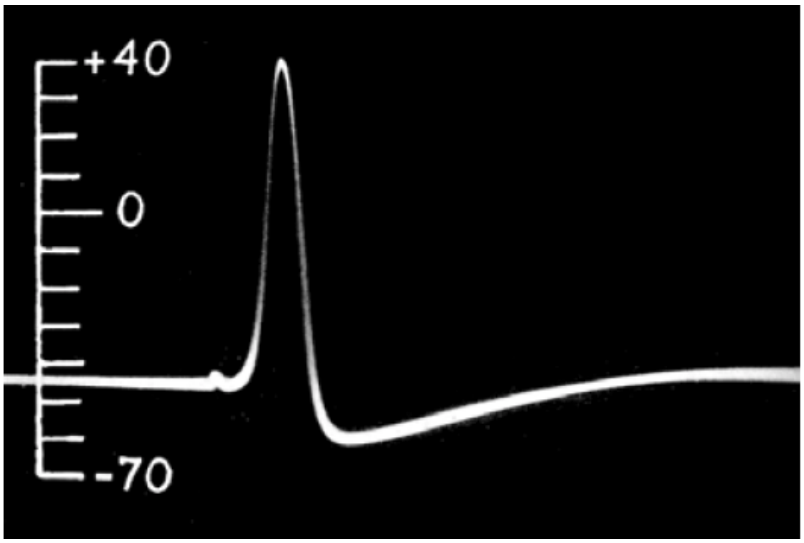

Figure 12: Action potential and resting potential recorded between the inside and outside of a giant axon. Source: [16].

6 Hodgkin & Huxley model of action potential propagation

6.1 Action potentials

In the previous sections, we looked at the very simplified model of a passive membrane. We solved the cable equation numerically and studied its results. Fig. 11 showed us behaviour that we would expect from a passive cable. Namely, the injected current can only travel a small distance along the axon before it has fully leaked out through the membrane. Furthermore, as soon as we stop injecting current, the membrane capacitance quickly discharges and drops the membrane potential back to its resting value. In this case, the membrane potential is characterized by a steady increase and a quick decrease back to rest.
However, Intracellular recordings (see Fig. 12) demonstrate that the membrane potential V_m is actually characterized by a sharp increase (**depolarization**) that reverses the potential sign, followed by a decrease back to the resting potential (**repolarization**). Before returning to the rest, the potential can drop under the resting value which we call **hyperpolarization**. We call these types of propagated signals **action potentials**.
What we would like to do now is to adjust our passive cable model such that we can describe and study these action potentials. For this we will follow the work of Hodgkin and Huxley [6] who were the first to provide a quantitative description of active membranes. These membranes contain ion channels that open or close depending on the membrane potential.

6.2 Active ion channels

In order to model the active properties of the membrane, we need to extend our passive membrane model of before and add active ion channels. These are channels that selectively open to ions depending on the membrane potential. Since the work of Hodgkin and Huxley, a large number of active channels have been discovered. However, we will only look at potassium and sodium channels as did Hodgkin and Huxley when studying the squid giant axon. Although there many more channels, the sodium and potassium currents are the major players in the propagation of action potentials and hence, this simplification is not that bad.
In Fig. 13, the equivalent circuit used by Hodgkin and Huxley is displayed. Instead of having a leaky membrane consisting of holes, we now have three types of ionic currents in the circuit:

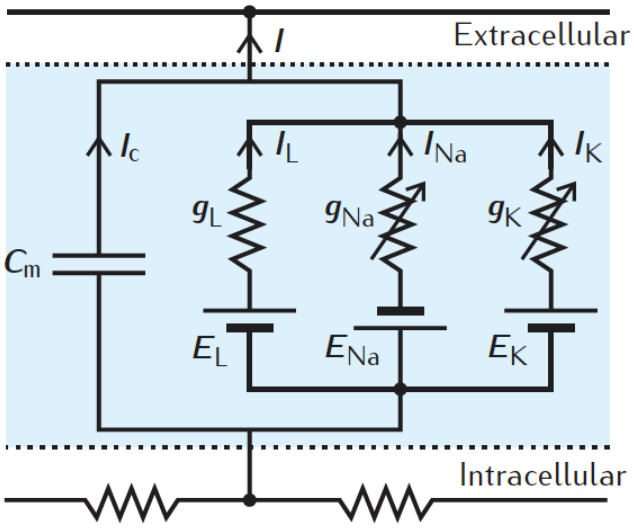

Figure 13: The Hodgkin-Huxley equivalent circuit. Source: [23].

A large potassium and sodium current, and a small leak current which will mostly consist of chloride ions. Note that the conductances of the sodium and potassium channels are variable and depend on voltage. This voltage dependence contains the active mechanism of the membrane. Just like before, we can write down expressions for the ionic currents in terms of their conductances as:

$$\begin{aligned} I_K &= g_K(V_m - E_K), \\ I_{Na} &= g_{Na}(V_m - E_{Na}), \\ I_L &= \bar{g}_L(V_m - E_L). \end{aligned} \tag{26}$$

Note that we put a bar over $\bar{g}_L$ which indicates that this is a constant unlike g_K and g_{Na} which depend on the voltage. In our discussion of the passive cable model, we worked with the departure from the resting potential given by $V = V_m - E_r$. Since in most works this is the standard choice, for practical reasons we would like to rewrite the equations for the ionic currents in terms of this potential as well. For this we define the potentials:

$$\begin{aligned} V_K &= E_K - E_r, \\ V_{Na} &= E_{Na} - E_r, \\ V_L &= E_l - E_r. \end{aligned} \tag{27}$$

Using these equations, we can then rewrite our current expressions to a more practical form given by:

$$\begin{aligned} I_K &= g_K(V - V_K) \\ I_{Na} &= g_{Na}(V - V_{Na}) \\ I_L &= \bar{g}_L(V - V_L). \end{aligned} \tag{28}$$

In order to use the equations above, we first need to find expression for the ionic conductances. Hodgkin and Huxley did this by fitting equations to experimental data. In the next sections, we will consider both the potassium and sodium currents and provide the relevant expressions which were obtained by Hodgkin and Huxley by fitting to data.

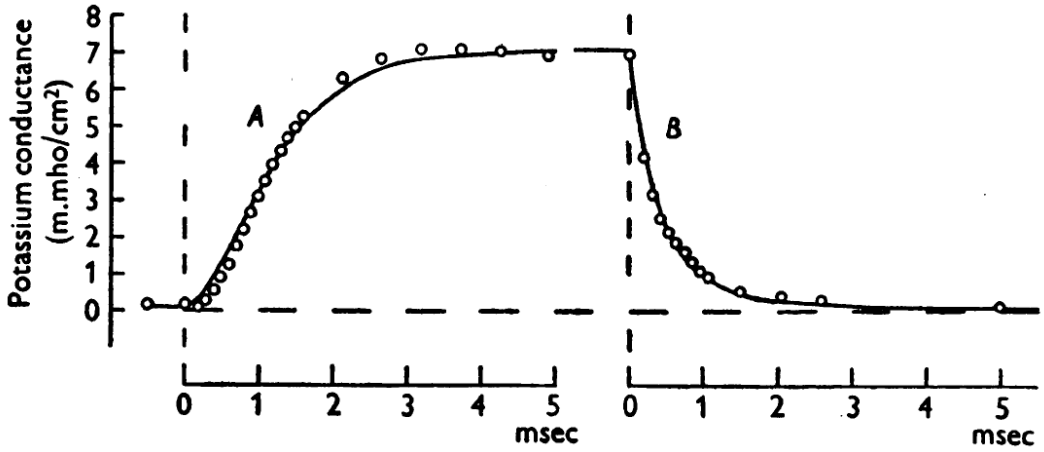

Figure 14: Time course of the potassium conductance. **A)** Rise of potassium conductance due to a depolarization of 25 mV. **B)** Fall of potassium conductance due to repolarization to the resting potential. The circles represent experimental data points obtained for a squid giant axon at a temperature of 21°C in choline sea water. The solid line is drawn according to eq (33) with the following parameters:
Curve A: $g_{K0} = 0.09$ m.mho/cm^2, $g_{K\infty} = 7.06$ m.mho/cm^2, $\tau_n = 0.75$ ms.
Curve B: $g_{K0} = 7.06$ m.mho/cm^2, $g_{K\infty} = 0.09$ m.mho/cm^2, $\tau_n = 1.1$ ms. Source: [6]

6.3 The potassium conductance

We mentioned before that the potassium and sodium conductances depend on the voltage. Before we look for their expressions however, we first show where this idea of voltage dependent conductances come from. By using voltage clamp experiments, Hodgkin and Huxley were able to measure the potassium conductance for a number of holding potentials for the squid giant axon. Some of the results they obtained are shown in Fig. 14, 15. All of these plots show similar behaviour, namely, by depolarizing the membrane, the potassium conductance increases until it has reached its peak value. After one drops the holding potential, the potassium conductance decays exponentially back to zero. Note here that although the depolarizations of 25 mV in Fig. 14 and 26 mV in Fig. 15 are almost the same, the rise of the first one is much faster. This is due to the fact that the first experiments were done at a temperature of 21°C while the second ones were done at a much colder temperature of 6°C.
By looking at the family of curves in Fig. 15, one can make the following observations:

- The peak conductance value $g_{K\infty}$, which is reached after some time, becomes larger if we increase the holding potential V. Furthermore, this increase slows down which means that there is a maximum value for the conductance which Hodgkin and Huxley named $\bar{g}_K$.
- By increasing the depolarization, the conductance rises faster to its peak value.

Hence, the results shown in Fig. 14, 15 show us that the conductance indeed depends on the voltage. Now that we have convinced ourselves of its voltage dependence, lets us turn to its expression. Hodgkin and Huxley tried a number of models to describe this voltage dependence. By considering the rise and fall of the data points in Fig. 14, they speculated that the rising phase of the conductance can be fitted by a third- or fourth-order equation while the drop can be fitted by a first-order equation. This idea can be simplified by assuming that g_K is proportional to the fourth power of a variable which obeys a first-order equation. The simplest

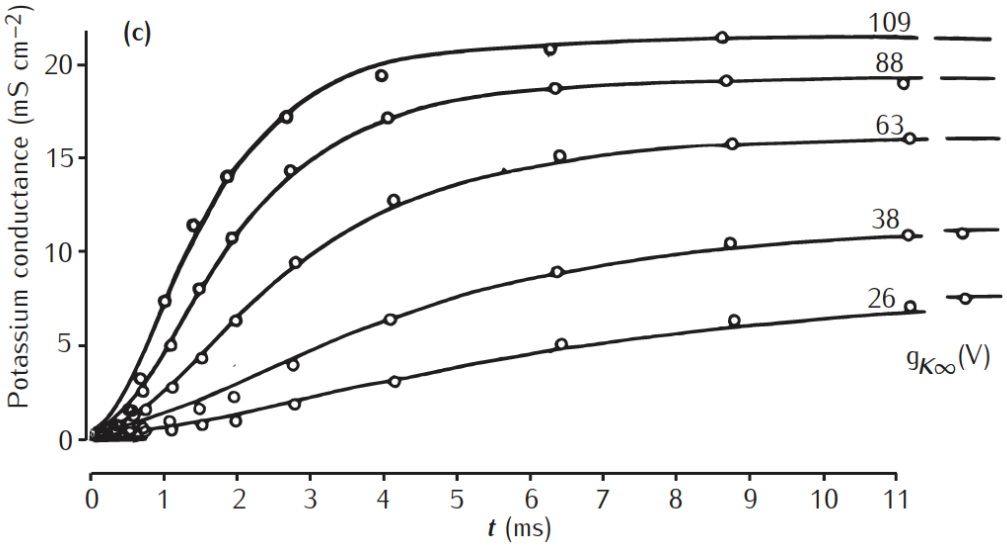

Figure 15: Rise of the potassium conductance associated with different depolarizations. The circles represent experimental data points obtained for a squid giant axon at temperatures between 6-7°C in choline sea water and sea water. The solid lines are drawn according to eq (33). Source: [23].

assumptions that provided the best fits to the data are:

$$\begin{aligned} g_K &= \bar{g}_K n^4 \\ \frac{dn}{dt} &= \alpha_n(1-n) - \beta_n n. \end{aligned} \tag{29}$$

Here $\bar{g}_K$ is the maximum conductance with dimensions of [conductance/cm^2], α_n and β_n [1/time] are rate constants which vary with voltage but not with time and n is a dimensionless variable which can vary between 0 and 1.
Now let us see if these equations do indeed provide a good fit to the data points. At rest, we have $dn/dt = 0$ which, when plugged into the rate equation above, gives us an expression for the resting value of n, denoted n_0:

$$n_0 = \frac{\alpha_{n0}}{\alpha_{n0} + \beta_{n0}}. \tag{30}$$

Using the boundary condition $n(0) = n_0$ we can solve the inhomogeneous linear differential equation (29) to obtain the following expression for n.

$$\begin{aligned} n &= n_\infty - (n_\infty - n_0)\exp(-t/\tau_n) \\ n_\infty &= \frac{\alpha_n}{\alpha_n + \beta_n} \\ \tau_n &= \frac{1}{\alpha_n + \beta_n} \end{aligned} \tag{31}$$

Finally, using the relations

$$\begin{aligned} g_{K\infty} &= \bar{g}_K n_\infty^4 \\ g_{K0} &= \bar{g}_K n_0^4 \end{aligned} \tag{32}$$

And the expression for n, we can rewrite eq (29) to the form

$$g_K = \{(g_{K\infty})^{1/4} - [(g_{K\infty})^{1/4} - (g_{K0})^{1/4}] \exp(-t/\tau_n)\}^4 \tag{33}$$

Where g_{K0} is the value of the conductance at $t = 0$ and $g_{K\infty}$ is the value which the conducatance finally attains. The solid lines shown in Fig. 14, 15 were calculated from eq (33) while using values for $g_{K\infty}$, g_{K0} and τ_n to get the best possible fit. One can clearly see the good agreement between the expression and the measurements.
Using these fits, we can determine the voltage dependence of the rate coefficients α_n and β_n. We start by rewriting the expressions for n_∞ and τ_n in eq (31) to the form:

$$\begin{aligned} \alpha_n &= n_\infty/\tau_n, \\ \beta_n &= (1 - n_\infty)/\tau_n. \end{aligned} \tag{34}$$

So after fitting eq (33) to the measurements, we can use the fit parameters n_∞ and τ_n to determine the values of α_n and β_n at that particular holding potential. In order to find the expressions for α_n and β_n as a function of the membrane potential V, Hodgkin and Huxley collected all the values of α_n and β_n from the fits in Fig. 14, 15 and plotted them against V. However, not all measurements which were used to calculate α_n, β_n were done at the same temperature. So in order to compare the different measurements, one needs to scale the values of the rate coefficients to the desired temperature. Hodgkin & Huxley used the Q10 temperature coefficient to do this. The Q10 coefficient is a measure of the rate of change of biological parameters as a consequence of increasing the temperature by 10°C. It is often used in biological systems to compare parameters at different temperatures and is given by the expression:

$$Q_{10} = (\frac{R_2}{R_1})^{10/(T_2 - T_1)}. \tag{35}$$

Where T_2, R_2 are the desired temperature and corresponding rate coefficient and T_1, R_1 are the temperature and corresponding rate coefficient which were measured. Hodgkin & Huxley found from measurements that they could compare measurements done at different temperatures by assuming a Q10 of 3 [7]. The results that they obtained for α_n and β_n are shown in Fig 16. Finally, Hodgkin and Huxley wrote down the simplest expressions for α_n and β_n that provide good fits to the data. These are given by:

$$\begin{aligned} \alpha_n &= 0.01(10 - V)/\Big[\exp\frac{10 - V}{10} - 1\Big], \\ \beta_n &= 0.125\exp(-V/80). \end{aligned} \tag{36}$$

To summarize, the set of equations that describe the potassium current for the squid giant axon are:

$$\begin{aligned} I_K &= g_K(V - V_K), \\ g_k &= \bar{g}_K n^4, \\ \frac{dn}{dt} &= \alpha_n(1 - n) - \beta_n n, \\ \alpha_n &= 0.01(10 - V)/\Big[\exp\frac{10 - V}{10} - 1\Big], \\ \beta_n &= 0.125\exp(-V/80). \end{aligned} \tag{37}$$

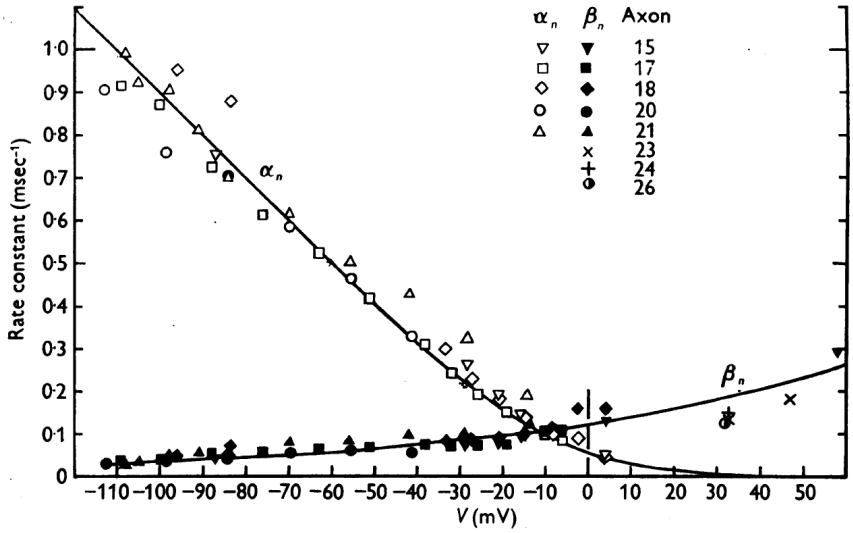

Figure 16: The potassium rate constants α_n and β_n as a function of the membrane potential. Here the empty shapes represent measurements of α_n while the filled shapes represent measurements of β_n. The different shapes represent measurements of different axons. Source: [6].

6.4 The sodium conductance

The expression for the sodium conductance was found in a similar way as the potassium conductance. We start off by considering a set of measurements done at different depolarizing holding potentials (see Fig. 17). Comparing with the behaviour of the potassium conductance in Fig. 14, we note that the major difference is that, even though we have not dropped the holding potential, the sodium conductance rises to its peak and then drops back to zero. This is unlike the potassium conductance which rises to its peak and remains there until the holding potential has been dropped. We call this fall of the sodium conductance **inactivation**. In order to quantify this inactivation process, Hodgkin and Huxley performed a range of voltage clamp experiments [8]. They then settled for the simplest description that would provide good fits to their experimental results. This description has two rate variables m and h to represent the level of activation and inactivation respectively, and the relevant equations are:

$$\begin{aligned} g_{Na} &= m^3 h \bar{g}_{Na}, \\ \frac{dm}{dt} &= \alpha_m(1-m) - \beta_m m, \\ \frac{dh}{dt} &= \alpha_h(1-h) - \beta_h h. \end{aligned} \tag{38}$$

Where $\bar{g}_{Na}$ is the maximum sodium conductance with dimensions of [conductance/cm^2] and $\alpha_m, \alpha_h, \beta_m$ and β_h [1/time] are rate coefficients which vary with voltage but not with time and m, h are dimensionless variables which can vary between 0 and 1.
Now we wish to see how well the equations above fit to the experimentally measured data. The solutions of the rate equations in (38) which satisfy the boundary conditions $m(0) = m_0$

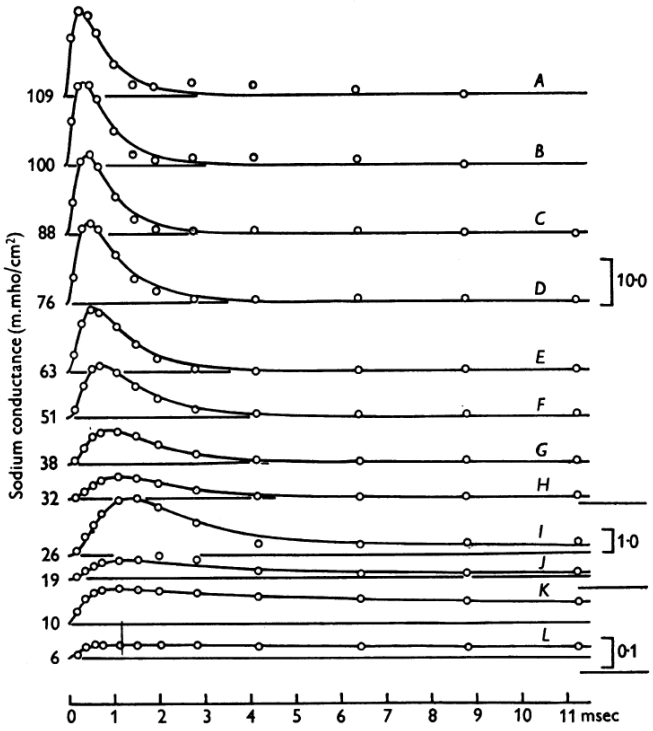

Figure 17: Rise and fall of the sodium conductance associated with different depolarizations. The circles are measurements took from a squid giant axon at temperatures of 6-7°C. The numbers to the left show the depolarization in mV while the scales on the right are given in m.mho/cm^2. Source: [6].

and $h(0) = h_0$ are

$$\begin{aligned} m &= m_\infty - (m_\infty - m_0)\exp(-t/\tau_m) \\ h &= h_\infty - (h_\infty - h_0)\exp(-t/\tau_h) \\ m_\infty &= \frac{\alpha_m}{\alpha_m + \beta_m} \\ \tau_m &= \frac{1}{\alpha_m + \beta_m} \\ h_\infty &= \frac{\alpha_h}{\alpha_h + \beta_h} \\ \tau_h &= \frac{1}{\alpha_h + \beta_h} \end{aligned} \tag{39}$$

By plugging these expressions for m and h into eq (38), one can can obtain an expression for g_{Na} as a function of time and the parameters $\bar{g}_{Na}, m_\infty, h_\infty, \tau_m, \tau_h, m_0, h_0$. Then, by using appropriate values for the parameters, this equation for g_{Na} can be compared to the measurements as shown by the solid lines in Fig. 17. One can see that the agreement is quite good.
After having fitted the theoretical curves to the data points, the voltage dependence of $\alpha_m, \alpha_h, \beta_m$

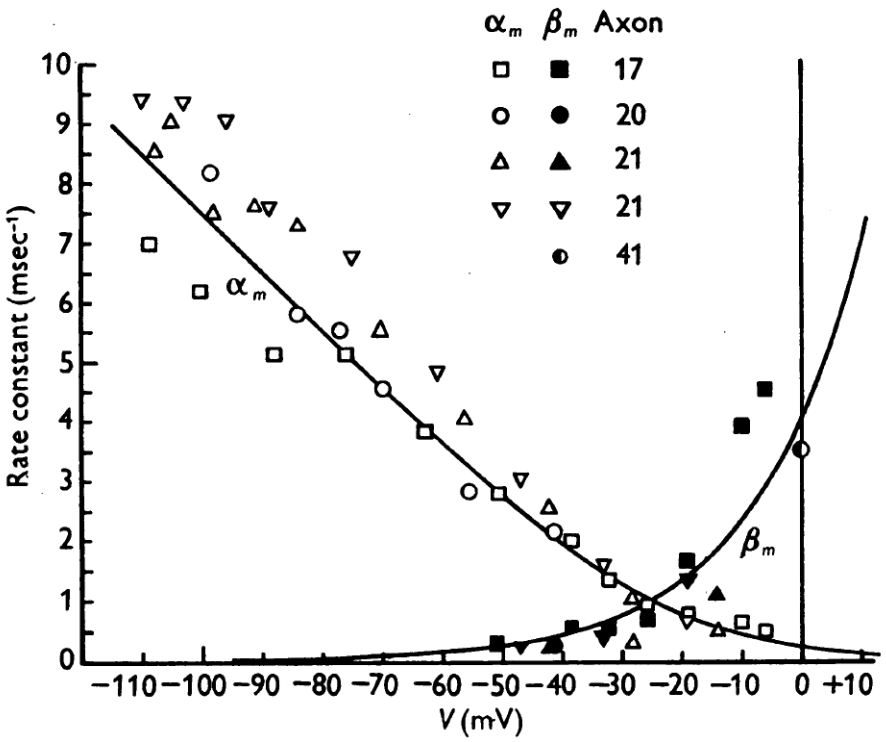

Figure 18: Rate coefficients α_m and β_m as a function of membrane potential. The points represent measurments while the solid lines are drawn according to eq (41). The measurements were done at temperatures between 3 and 11°C, but were scaled to 6°C using a temperature coefficient (Q10) of 3. Source: [6].

and β_h can be determined similar to the case for potassium by using:

$$\begin{aligned} \alpha_m &= m_\infty/\tau_m, \\ \beta_m &= (1-m_\infty)/\tau_m \\ \alpha_h &= h_\infty/\tau_h, \\ \beta_h &= (1-h_\infty)/\tau_h. \end{aligned} \tag{40}$$

Using the fit parameters, Hodgkin and Huxley collected the values of $\alpha_m, \beta_m, \alpha_h$ and β_h from different experiments and plotted them against the holding potential in Fig. 18 and 19. They then wrote down equations for $\alpha_m, \beta_m, \alpha_h$ and β_h in terms of the potential V that would provide the best fit to the data and settled for the following equations which are represented as solid lines in Fig. 18 and 19:

$$\begin{aligned} \alpha_m &= 0.1(25-V)/(\exp\frac{25-V}{10}-1), \\ \beta_m &= 4\exp(-V/18), \\ \alpha_h &= 0.07\exp(-V/20), \\ \beta_h &= 1/(\exp\frac{30-V}{10}+1). \end{aligned} \tag{41}$$

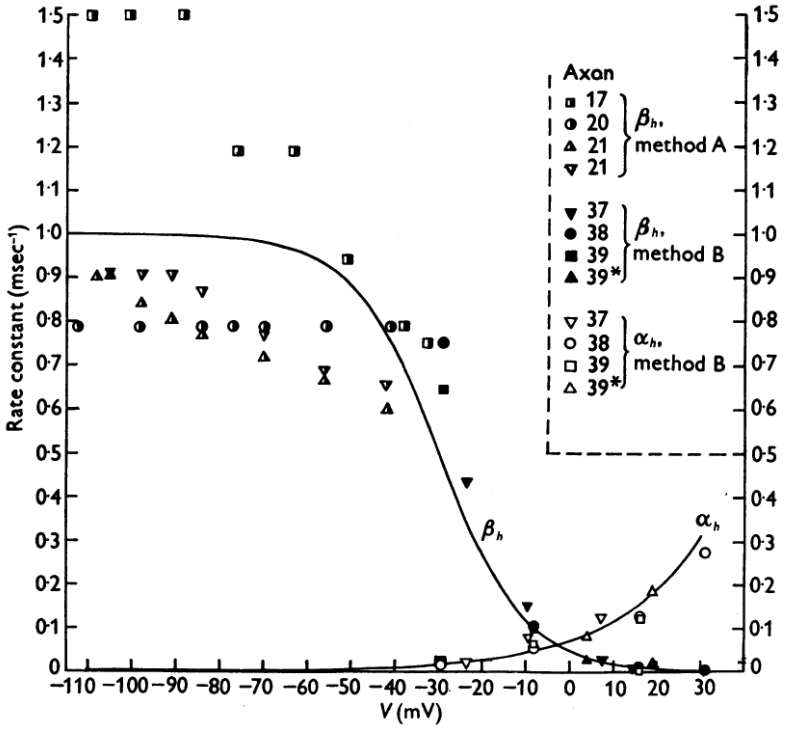

Figure 19: The rate coefficients of inactivation α_h and β_h as a function of the membrane potential. The points represent measurements while the solid lines are drawn according to eq (41). Not all of the measurements where done at the same temperature, but they were scaled to 6°C by using a temperature coefficient of 3. Source: [6].

To summarize, the set of equations that describe the sodium current for the squid giant axon are given by:

$$
\begin{aligned}
I_{Na} &= g_{Na}(V - V_{Na}), \\
g_{Na} &= \bar{g}_{Na} m^3 h, \\
dm/dt &= \alpha_m(1-m) - \beta_m m, \\
dh/dt &= \alpha_h(1-h) - \beta_h h, \\
\alpha_m &= 0.1(25-V)/(\exp\frac{25-V}{10} - 1), \\
\beta_m &= 4\exp(-V/18), \\
\alpha_h &= 0.07\exp(-V/20), \\
\beta_h &= 1/(\exp\frac{30-V}{10} + 1).
\end{aligned}
\tag{42}
$$

6.5 The active cable model

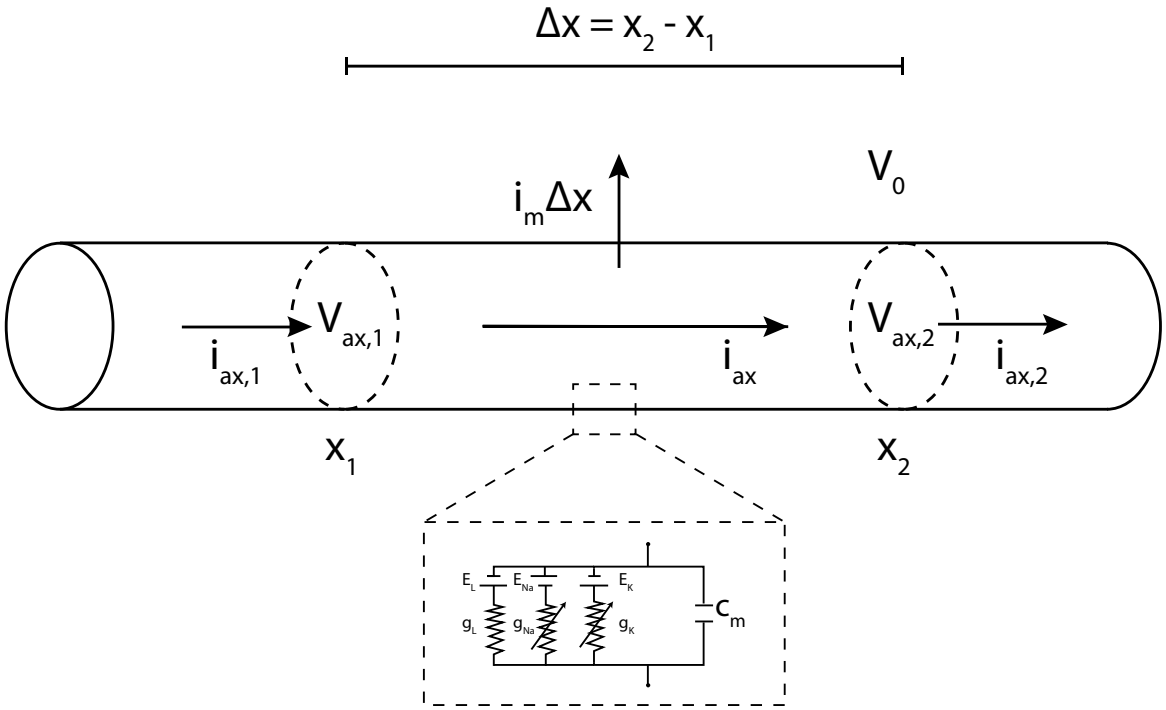

Figure 20: Schematic drawing of the active cable with variable potassium and sodium conductances.

Having determined the voltage dependent expressions for the sodium and potassium conductances, we now wish to combine everything together to form an active cable model that describes action potential propagation in axons. Luckily, We have already done most of the work in our derivation of the passive cable equation. The only thing that we need to do is change the passive membrane from before to an active membrane consisting of variable conductances. See Fig. 20 for a drawing of a segment of an axon with active membrane components.
In our derivation of the passive cable equation, we found the following expression for the membrane currents:

$$\frac{1}{r_{ax}}\frac{\partial^2 V}{\partial x^2} = i_m \tag{43}$$

Where i_m [μA/cm] is the outward membrane current per unit length, $V = V_m - E_r$ [mV] is the departure of the membrane potential from its resting value and r_{ax} [kΩ/cm] is the axon core resistance per unit length.
We first rewrite this in more conventional units by using the relations:

$$\begin{aligned} r_{ax} &= \frac{4R_{ax}}{\pi d^2}, \\ i_m &= \pi d I_m. \end{aligned} \tag{44}$$

Here R_{ax} [kΩ cm] is the axon core resistivity and I_m [μA/cm^2] is the membrane current density. Using these relations, we rewrite the equation above in the following form:

$$\frac{d}{4R_{ax}}\frac{\partial^2 V}{\partial x^2} = I_m. \tag{45}$$

In the active cable model, the membrane current is the combination of potassium, sodium, leak and capacitive currents. Using the expressions for the potassium and sodium currents that we found in the previous sections, we can write the membrane current as:

$$I_m = C_m \frac{\partial V}{\partial t} + \bar{g}_L(V - V_L) + \bar{g}_K n^4 (V - V_K) + \bar{g}_{Na} m^3 h (V - V_{Na}) \tag{46}$$

Where C_m [μF/cm^2] is the specific membrane capacitance. Combining the two equations above, we arrive at the Hodgkin and Huxley active cable equation:

$$\frac{d}{4R_{ax}} \frac{\partial^2 V}{\partial x^2} = C_m \frac{\partial V}{\partial t} + \bar{g}_L(V - V_L) + \bar{g}_K n^4 (V - V_K) + \bar{g}_{Na} m^3 h (V - V_{Na}) \tag{47}$$

With the potassium and sodium rate variables given by:

$$\begin{aligned} \frac{dn}{dt} &= \alpha_n(1-n) - \beta_n n, \\ \alpha_n &= 0.01(10-V)/\Big[\exp\frac{10-V}{10} - 1\Big], \\ \beta_n &= 0.125\exp(-V/80). \end{aligned} \tag{48}$$

$$\begin{aligned} \frac{dm}{dt} &= \alpha_m(1-m) - \beta_m m, \\ \frac{dh}{dt} &= \alpha_h(1-h) - \beta_h h, \\ \alpha_m &= 0.1(25-V)/(\exp\frac{25-V}{10} - 1), \\ \beta_m &= 4\exp(-V/18), \\ \alpha_h &= 0.07\exp(-V/20), \\ \beta_h &= 1/(\exp\frac{30-V}{10} + 1), \end{aligned} \tag{49}$$

Now that we have a full quantitative description of the active membrane, we turn to numerically solving the above equations and studying the results. First of all, we would like to see whether the above equations can indeed reproduce measurements. If the agreement turns out to be good, we will analyze the conductances and currents in order to understand the process behind action potential propagation.

7 Numerical solution of the Hodgkin & Huxley equations

In section 9, we provide the discretization and numerical procedure that we used to solve the Hodgkin & Huxley equations. Just like in the passive cable case, we initiate our system by injecting a current at $x = 0$ for a certain amount of time (see 10) while keeping the ends sealed by eq (69). The parameters that we used for the simulations are those for the squid giant axon provided by Hodgkin & Huxley [6]. They are given by:

$$\begin{aligned} d &= 476\ \mu\text{m} \\ R_{ax} &= 35.4\ \Omega\text{cm} \\ C_m &= 1\ \mu\text{F/cm} \end{aligned} \tag{50}$$

$$\begin{aligned} g_{Na} &= 120\ \text{mS/cm}^2 \\ g_K &= 36\ \text{mS/cm}^2 \\ g_L &= 0.3\ \text{mS/cm}^2 \\ V_{Na} &= 115\ \text{mV} \\ V_K &= -12\ \text{mV} \\ V_L &= 10.613\ \text{mV} \end{aligned} \tag{51}$$

We choose our dimensions such that the length and time of the cable is long enough for us to be able to study the propagation of the action potentials while not having too long simulation

times.

$$\begin{aligned} L &= 50 \text{ cm} \\ \Delta x &= 0.05 \text{ cm} \\ T &= 50 \text{ ms} \\ \Delta t &= 0.005 \text{ ms} \end{aligned} \tag{52}$$

In order to study the action potentials at different temperatures, Hodgkin & Huxley scaled the rate coefficients α_y, β_y for $y = n, m, h$ by multiplying them with a Q10 coefficient of 3. The rest of the parameters were chosen to be independent of temperature [6]. By using the above set of parameters and scaling the rate coefficients with a Q10 of 3, we solved the Hodgkin & Huxley equations at different temperatures.

Let us start by considering action potentials at a low temperature of 9.1°C. These are in fact temperatures in which the squid giant axon naturally resides. The results are shown in Fig. 21. We can see that the agreement between our simulation of the Hodgkin & Huxley equations with measurement is quite good. The forms, amplitudes and time-scales are very much in agreement with each other. Our calculated action potential does however differ from the experimental one in the following ways: 1) Our potential drops slower. 2) The peak is sharper. and the end of the falling phase is sharper. These differences could be caused by our numerical procedure but we will not delve into this here since the agreement is good enough for the purpose of our study.

Our result at a temperature of 9.1°C showed a long return to rest which took around 12 ms. This is to be expected since we are considering quite low temperatures. We would then expect the duration of the action potential to decrease if we increase the temperature. We have done this by solving the Hodgkin & Huxley equations at a temperature of 20.5 °C. The results are shown in 22. Again we can see the agreement with experiment. As expected, the rise of the temperature has greatly reduced the duration of the action potential. Furthermore, it has lowered the amplitude by a small amount. Hence, by increasing the temperature, we get faster and slightly weaker action potentials.

Having convinced ourselves that our solutions of the Hodgkin & Huxley equations agree with experiments, we now turn to studying the various properties of action potentials. We started by plotted the action potential for different initial depolarizations (see Fig. 23). We observe that there is a threshold potential below which no action potential gets initiated. Instead the signal then just dissipates passively. When we increase the initial depolarization above the threshold, an action potential is initiated and propagates along the axon. Hence, the action potential is an all-or-nothing response.

Furthermore, if we try depolarizing the membrane during the hyperpolarizing phase (see Fig. 24), we observe that no action potential gets initiated. This means that during this phase, the membrane is not primed for another action potential. We call this phase of the action potential the refractory period. This property ensures that action potentials cannot propagate backwards.

Now let us look at the propagated action potential. In Fig. 25, we plotted the membrane potential ,with different initial stimuli, as a function of time at various points along the axon. From these results, we make the following observations: 1) The action potential moves down the axon at a constant speed. Which in Fig. 25 comes down to roughly 15 m/s. 2) The time course of each action potential is the same. 3) The peak is independent of the distance traveled (action potential preserves shape). 4) Above threshold stimuli create a propagating action potential whose amplitude is independent of the strength of the initial stimulus.

Now that we have seen the long-distance signal transmission of the action potential, we take a point along the axon and study the ionic currents at this point when an action potential passes. In Fig. 26, we have plotted the membrane potential, conductances and currents as a function

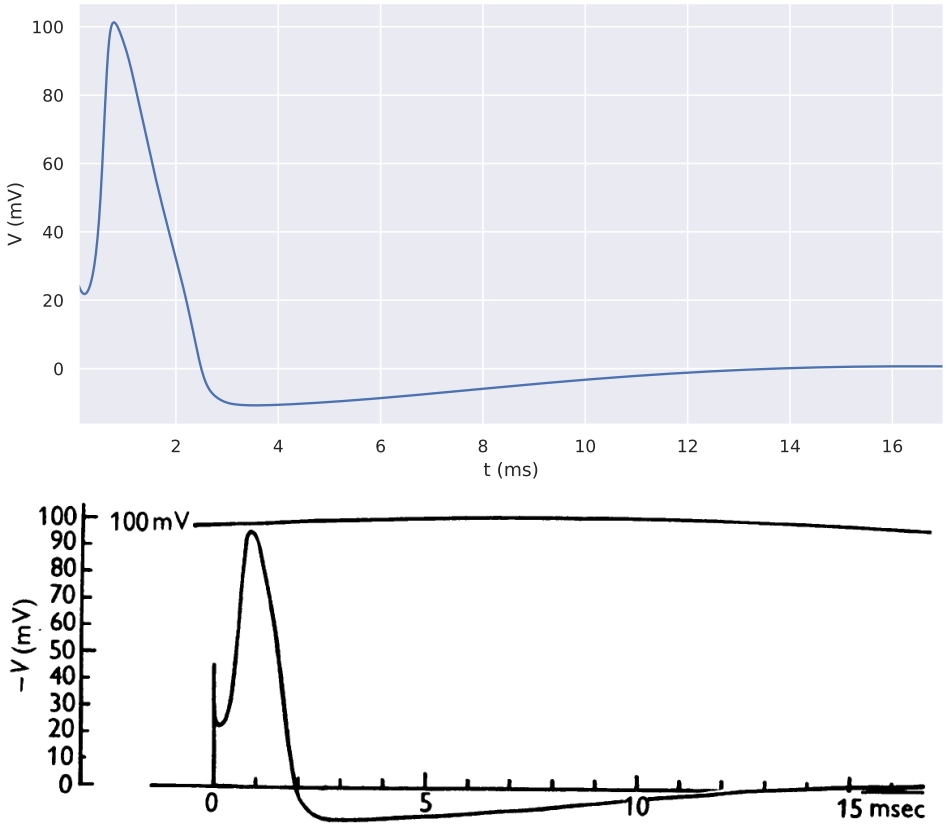

Figure 21: Top: Calculated action potential using the HH equations with the set of parameters given in eq (50) and (51) for a temperature of 9.1 °C. Bottom: Membrane potential recorded at T=9.1 °C, Source: [6].

of time at position $x = 15$ cm when an action potential passes. By looking at the conductances and the ionic currents, we can separate the action potential in the following 3 phases: **Phase 1)** As soon as the membrane potential passes its threshold value, The sodium conductance shoots up. This means that the channels open up causing sodium ions to flow into the axon which rapidly increases the membrane potential. This keeps going until the Membrane potential has reached its peak value. **Phase 2)** After the membrane potential has reached its peak value, the sodium conductance drops while the potassium conductance starts rising. This means that during this phase the sodium channels close while the potassium channels open causing a flow of potassium ions out of the axon. Potassium ions keep flowing out until the membrane potential has reached its rest value again. **Phase 3)** A excess outflow of positive charge can causes the membrane potential to drop below its resting value before it slowly returns to rest. A graphical summary of the flow of ionic currents during the propagation of an action potential is provided in Fig. 27.

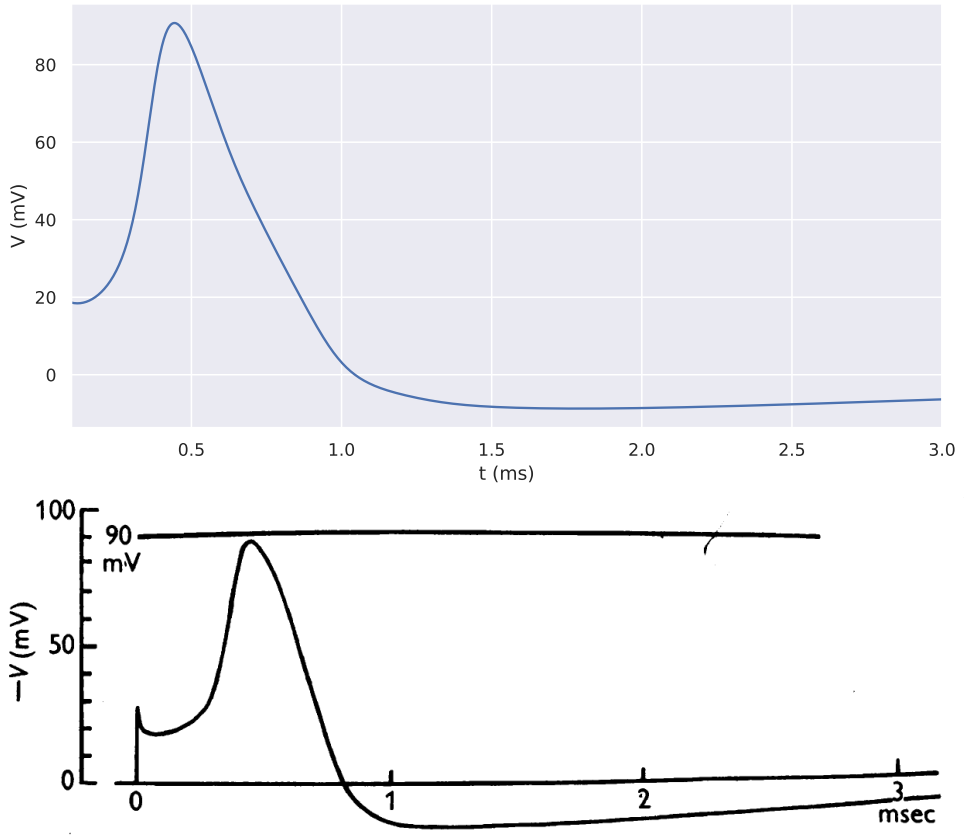

Figure 22: Top: Calculated action potential using the HH equations with the set of parameters given in eq (50) and (51) for a temperature of 20.5 °C. Bottom: Membrane potential recorded at T=20.5 °C, Source: [6].

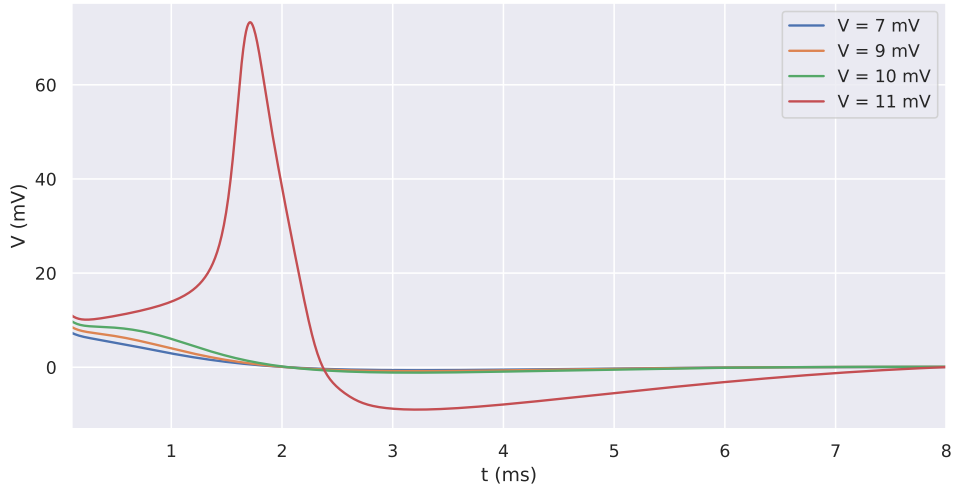

Figure 23: Solutions of the HH equations for different initial depolarizations. The simulations were done at a temperature of 18.5 °C and the system was initiated by injecting currents at $x = 0$ for 0.1 ms such that the membrane depolarizes to the desired value. Below the threshold potential of around 11 mV, initiations do not cause an action potential to emerge.

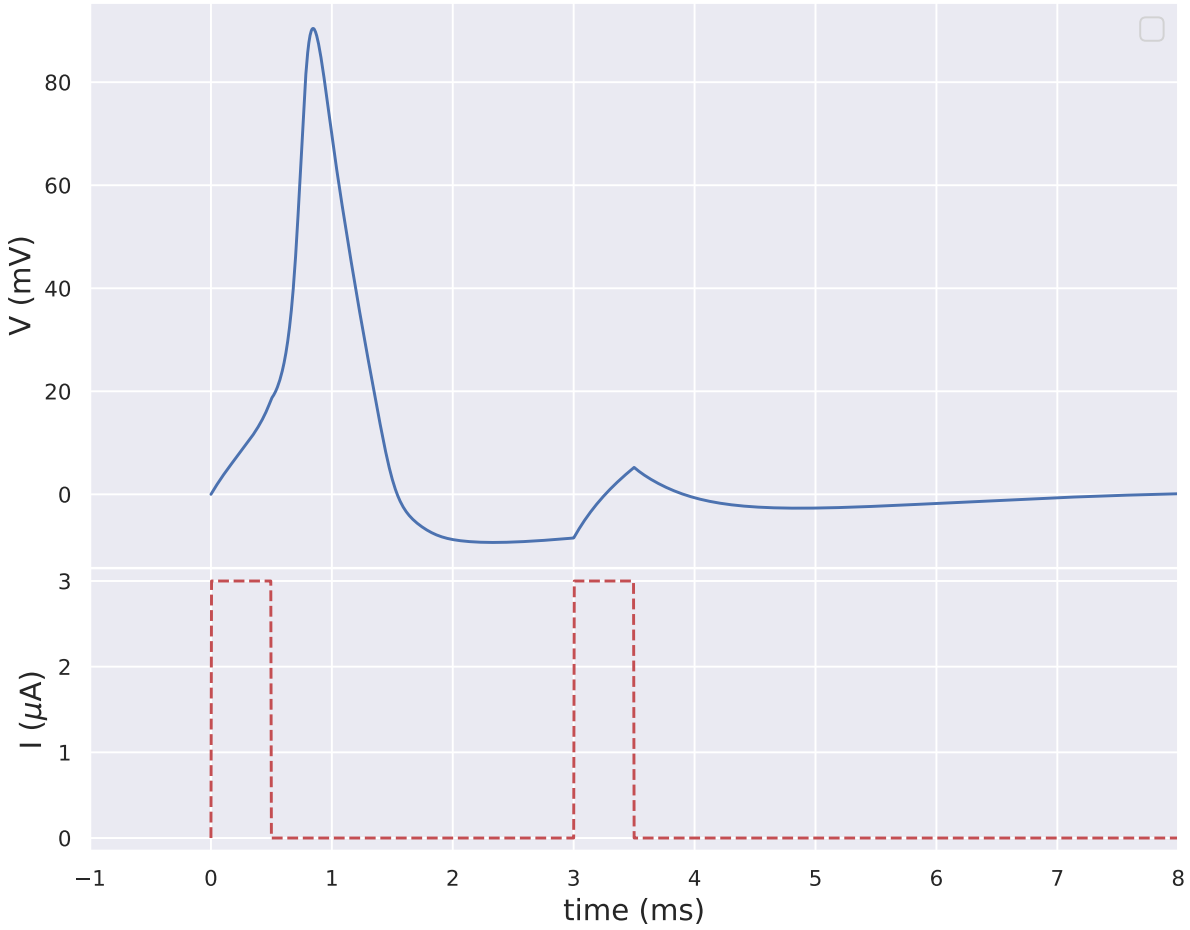

Figure 24: Results showing the refractory period in which the membrane is less likely to initiate another action potential. Two identical currents have been injected at different times. One at the beginning and one during the refractory period. We see that During the refractory period, the membrane is not primed for another action potential and the signal progresses passively instead. Temperature was set to 18.5 °C.

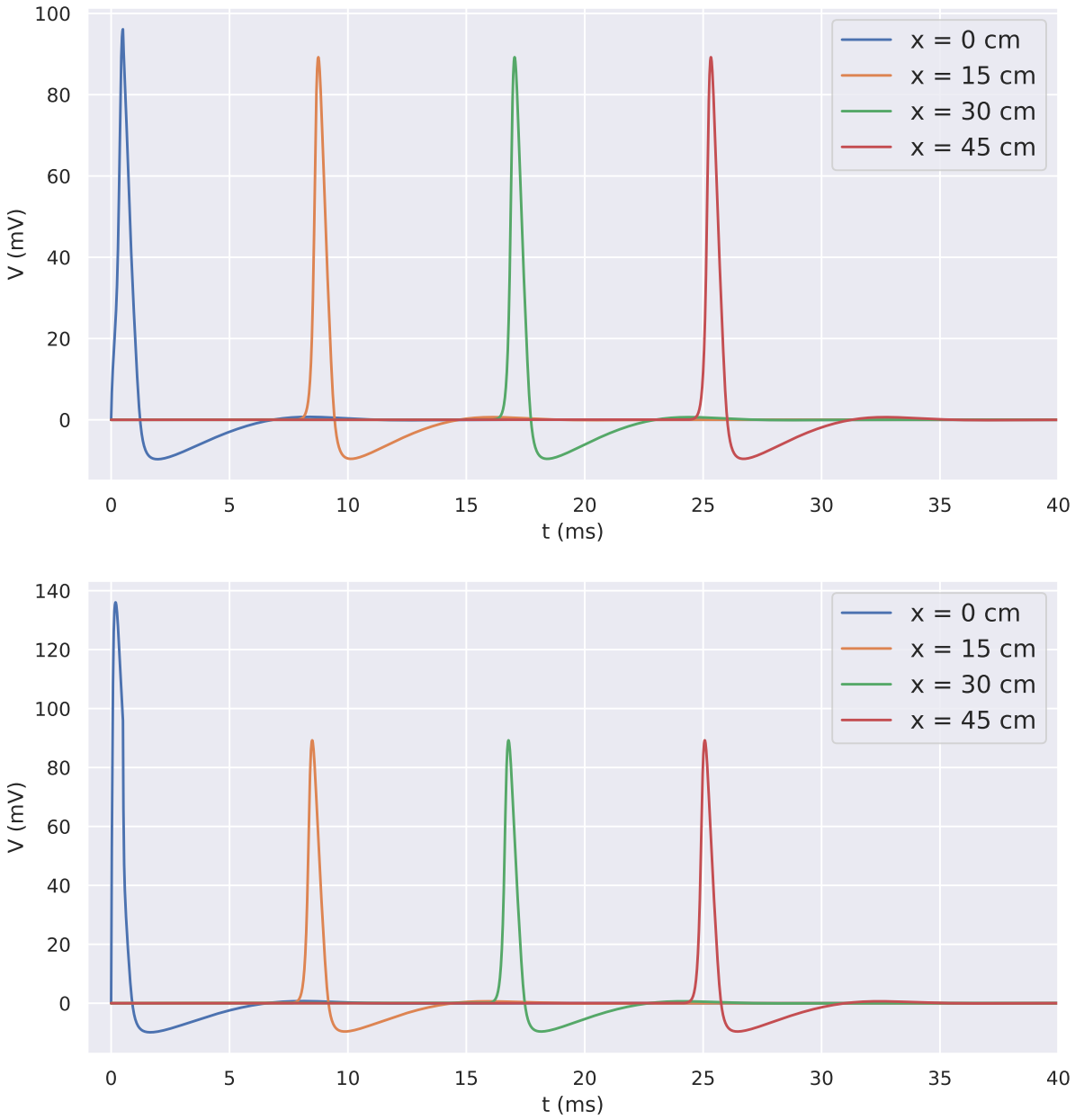

Figure 25: Solutions of the HH equations for different initiation strengths. In the top figure we injected 5 μA for 0.5 ms while in the bottom figure we injected 40 μA for 0.5 ms. It is clear that the propagated action potential does not depend on the initiation strength.

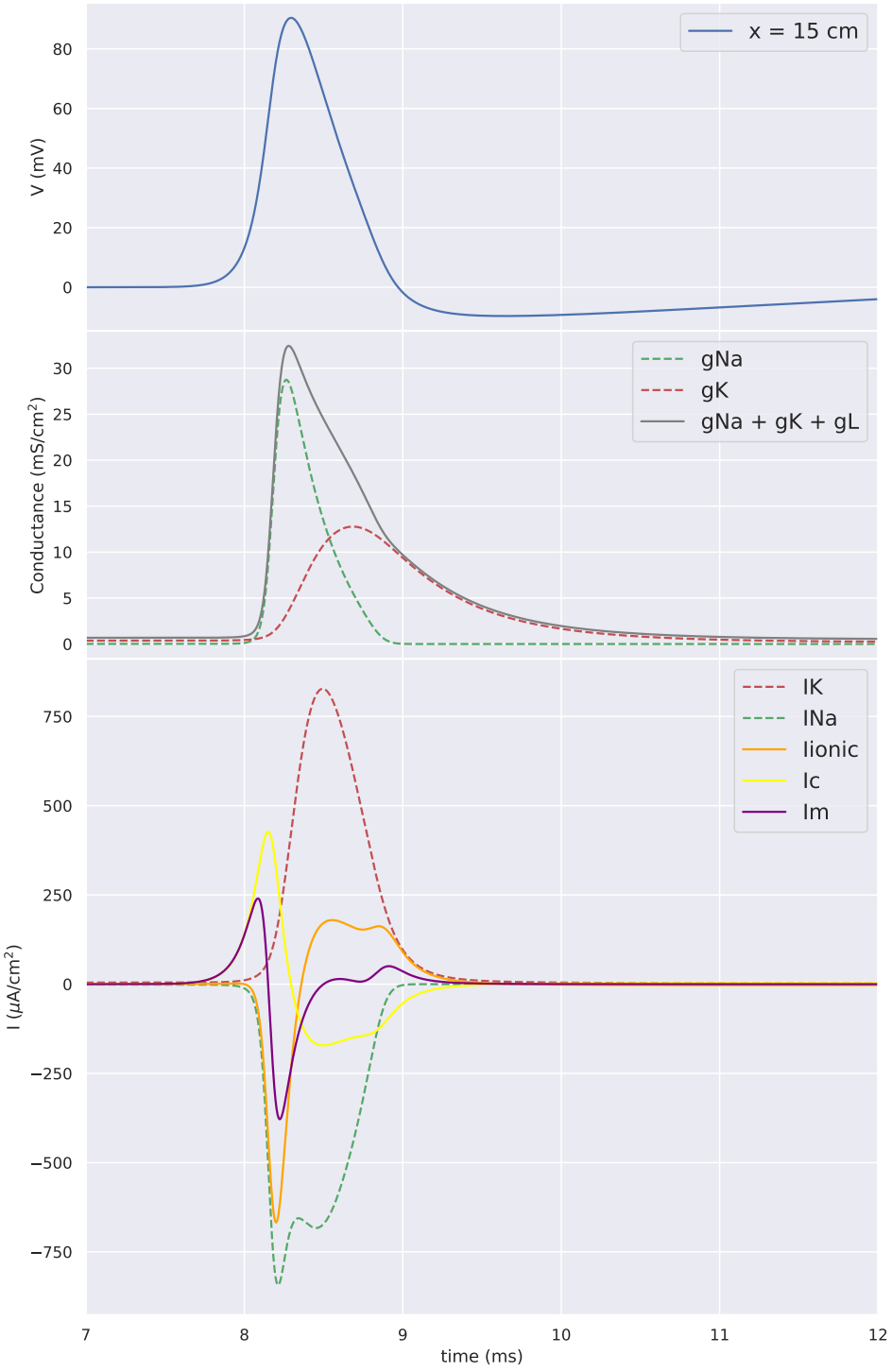

Figure 26: **Top:** Membrane potential as a function of time taken at $x = 15$cm. **Middle:** The sodium, potassium and total conductance as a function of time. **Bottom:** Current densities as a function of time. Potassium I_K, sodium I_{Na}, ionic $I_{ionic} = I_K + I_{Na}$, capacitive I_c and membrane $I_m = I_c + I_{ionic}$. The temperature was set to 18.5 °C.

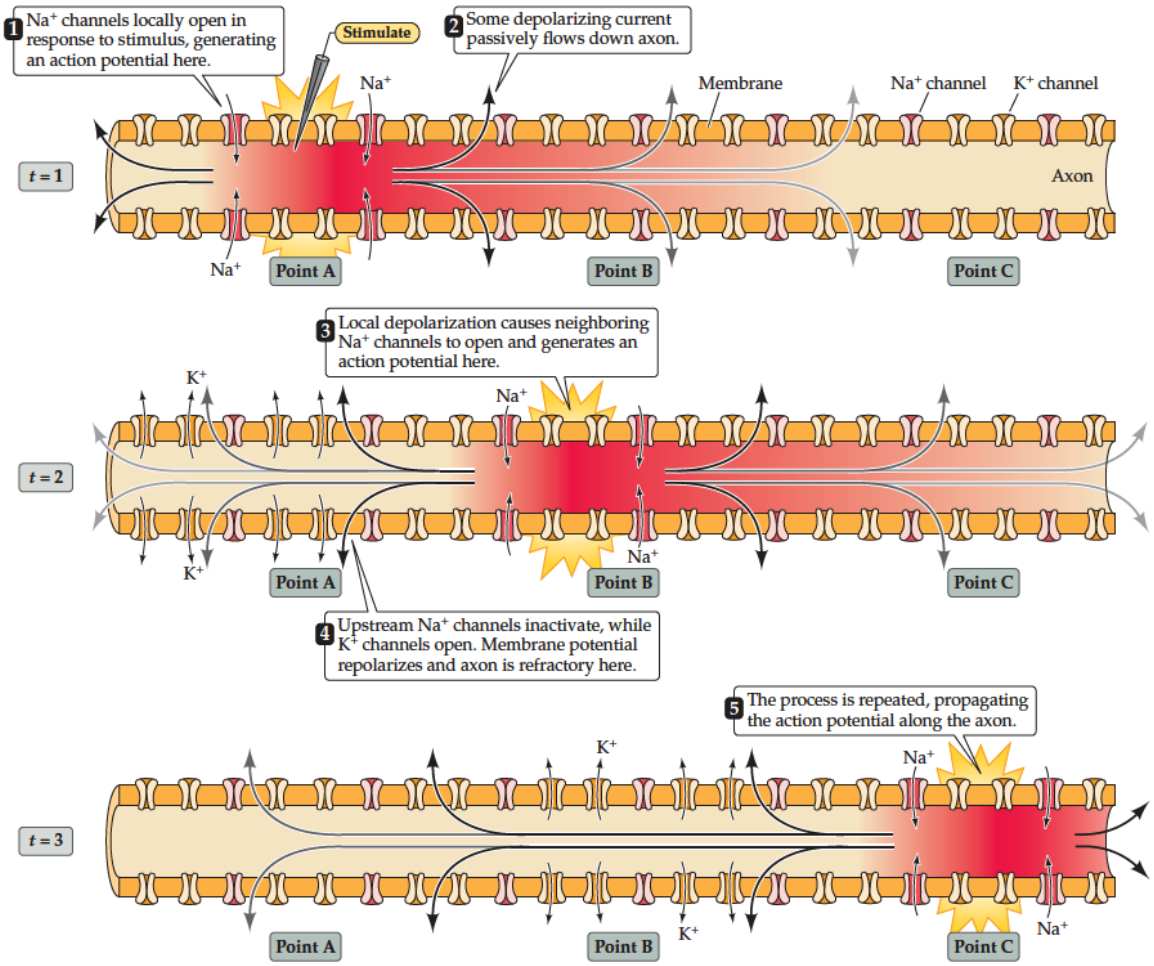

Figure 27: The active and passive current flows due to a passing action potential. Depolarization opens Na+ channels locally and produces an action potential at point A of the axon (time t = 1). The resulting inward current flows passively along the axon, depolarizing the adjacent region (point B) of the axon. At a later time (t = 2), the depolarization of the adjacent membrane has opened Na+ channels at point B, resulting in the initiation of the action potential at this site and additional inward current that again spreads passively to an adjacent point (point C) farther along the axon. At a still later time (t = 3), the action potential has propagated even farther. This cycle continues along the full length of the axon. Note that as the action potential spreads, the membrane potential repolarizes due to K+ channel opening and Na+ channel inactivation, leaving a "wake" of refractoriness behind the action potential that prevents its backward propagation. Source: [18].

8 Discussion and outlook

With the results that we obtained for the propagated action potential, we are ready to conclude this thesis. We set out to understand the propagation of signals through neurons and to find a model that could describe them by means of simple principles. After introducing the neuron and in particular the axon, we approached these questions by first working towards a cable model that could describe the passive flow of current in axons. For this model, the equivalent circuit representation of the cellular membrane was crucial. After studying the passive flow of current in axons, we extended the model to account for active currents by following the work of Hodgkin & Huxley [6]. This lead us to the Hodgkin & Huxley model which is an active cable model that describes the propagation of action potentials in excitable cells. For this one assumes that the membrane consists of voltage dependent ion channels that selectively open depending on the membrane potential. We then solved the Hodgkin & Huxley equations numerically and studied the propagated action potential. Form our results we found that the action potential has the following properties:

- They require a combination of active and passive currents.
- A threshold potential needs to be reached in order to initiate an action potential. This means that the action potential is an all-or-nothing response and hence is not graded.
- The regenerative property of the voltage-gated channels ensure long-distance transmission of electrical signals at constant speed.
- Following an action potential, there is a period in which the membrane is not primed for excitation. This is called the refractory period and it limits the number of action potentials that can be produced. Furthermore, it ensures that signals do not move backwards.

So we managed to model the propagation of signals in excitable cells and study its properties. However, this is only the beginning for there are still many questions left unanswered of whom I will mention a few here in the form of an outlook.
For instance, from our results we found that the conduction velocity was actually quite low (15 m/s for the squid giant axon at 18.5 °C). This is definitely not fast enough for most animals that require fast reaction. So then what causes the fast propagation of signals through axons? Recall that action potential conduction requires both active and passive flow of current. In order to speed up the conduction velocity, the passive flow of current along the axon needs to be improved. One way of doing this is by increasing the axon diameter, which will effectively lower the core resistance and increase the conduction velocity. Another way to improve the passive flow of current, which is the more efficient strategy, is to insulate the axonal membrane. This will reduce the leaking of current and hence increase the distance that the signal can flow passively. In most organisms, the conduction velocity is increased by insulating the axon with myelin [15]. Myelinated axons can conduct action potentials at velocities up to 120 m/s which is often 100 times faster than unmyelinated axons [18]. The idea behind it is saltatory conduction [24, 27]. Due to periodic gaps between myelin sheets, the time consuming process of action potential generation only occurs at specific points along the axon called the nodes of Ranvier (see Fig. 1). Studying this process called saltatory conduction and its precise effects on the propagation of action potentials in axons is something that we were unable to do in the amount of time available. Hence, this is an area which yet holds unanswered questions and worth pursuing.
There is another area of interest which is connected to myelin. The theory of saltatory conduction assumes that the myelin sheets act as insulators through which no currents can leak out. However, evidence has been found that the myelin sheets are in fact no perfect insulators but

instead contain a small pathway between the myelin and the axon core called the periaxonal space through which current can flow [2]. Double cable models have proposed to account for this leakage pathway by extending the familiar single cable model and assigning a voltage to the periaxonal space [1, 3, 4, 5, 11, 22]. The precise function and effects of this periaxonal space on the propagation of action potentials is something which is yet an active area of research with many unanswered questions.
Finally I wish to mention a topic that concerns the cable model description. Namely, The cable model which is widely used to describe the propagation of action potentials in axons has its flaws. Some of them are:

- The model assumes that ionic concentrations are not significantly altered by changes in conductivity due to changes in membrane permeability. Hence the assumption is that the equilibrium potentials do not change and remain fixed in the battery. However, there are cases where this is not a good assumption to make. For instance if the intracellular volume is relatively small, as in dendritic spines, then ionic concentrations tend to vary significantly due to changes in ionic conductance. Furthermore, in certain systems the ionic concentration on one side can change by orders of magnitude in milliseconds, causing a concentration gradients [21].

- In the cable model the driving force for the ionic current inside the cytoplasm is the potential gradient. However, driving forces caused by large concentration gradients are not incorporated. This could cause errors for small compartments like dendritic spines where large concentration gradients occur.

- Another limitation is the fact that the cable model considers the total cytoplasmic resistivity. This can cause errors when different ions have different concentration-dependent cytoplasmic resistivities. Since then large concentration gradients will cause the total resistivity to be a bad approximation.

Hence, another topic that one could pursue is to try and account for the above mentioned problems by considering electro-diffusion models [21, 25, 12, 14, 13, 17, 20, 9]. Clearly, in the study of nerve signal propagation there is still a lot of exciting things to pursue. In my time studying this field, I only scratched the surface of a very complex and interesting area of research which I personally will closely follow from now on.

References

[1] F. Awiszus. Effects of paranodal potassium permeability on repetitive activity of mammalian myelinated nerve fiber models. *Biol. Cybern.*, 64:69–76, 1990.

[2] E.F. Barrett and J.N Barrett. Intracellular recording from vertebrate myelinated axons: mechanism of the depolarizing afterpotential. *J. Physiol*, 323:117–144, 1982.

[3] A.R. Blight. Computer simulation of action potentials and afterpotentials in mammalian myelinated axons: the case for a lower resistance myelin sheath. *Neuroscience*, 15:13–31, 1985.

[4] A.R. Blight and S. Someya. Depolarizing afterpotentials in myelinated axons of mammalian spinal cord. *Neuroscience*, 15:1–12, 1985.

[5] H. Bostock, M. Baker, and G. Reid. Changes in excitability of human motor axons underlying post-ischaemic fasciculations: evidence for two stable states. *Journal of Physiology*, 441:537–557, 1991.

[6] A.L. Hodgkin and A.F. Huxley. A quantitative description of membrane current and its application to conduction and excitation in nerve. *J. Physiol*, 117:500–544, 1952.

[7] Alan L Hodgkin, Andrew F Huxley, and B Katz. Measurement of current-voltage relations in the membrane of the giant axon of loligo. *The Journal of physiology*, 116(4):424–448, 1952.

[8] Allan L Hodgkin and Andrew F Huxley. The dual effect of membrane potential on sodium conductance in the giant axon of loligo. *The Journal of physiology*, 116(4):497–506, 1952.

[9] Benzhuo Lu, Michael J Holst, J Andrew McCammon, and YC Zhou. Poisson–nernst–planck equations for simulating biomolecular diffusion–reaction processes i: Finite element solutions. *Journal of computational physics*, 229(19):6979–6994, 2010.

[10] M. Mascagni and A.S. Sherman. Numerical methods for neuronal modeling. 1989.

[11] Cameron C. Mcintyre, Andrew G. Richardson, and Warren M. Grill. Modeling the excitability of mammalian nerve fibers: Influence of afterpotentials on the recovery cycle. *J Neurophysiol*, 87:995–1006, 2002.

[12] Yoichiro Mori. From three-dimensional electrophysiology to the cable model: an asymptotic study. *arXiv preprint arXiv:0901.3914*, 2009.

[13] Yoichiro Mori, Glenn I Fishman, and Charles S Peskin. Ephaptic conduction in a cardiac strand model with 3d electrodiffusion. *Proceedings of the National Academy of Sciences*, 105(17):6463–6468, 2008.

[14] Yoichiro Mori and Charles Peskin. A numerical method for cellular electrophysiology based on the electrodiffusion equations with internal boundary conditions at membranes. *Communications in Applied Mathematics and Computational Science*, 4(1):85–134, 2009.

[15] Klaus-Armin Nave and Hauke B Werner. Myelination of the nervous system: mechanisms and functions. *Annual review of cell and developmental biology*, 30:503–533, 2014.

[16] Philip Nelson. *Biological physics: energy, information, life*. 2002.

[17] Jurgis Pods, Johannes Schönke, and Peter Bastian. Electrodiffusion models of neurons and extracellular space using the poisson-nernst-planck equations—numerical simulation of the intra-and extracellular potential for an axon model. *Biophysical journal*, 105(1):242–254, 2013.

[18] D. Purves et al. *Neuroscience 6th Edition*. Sinauer Associates, 2017.

[19] W. Rall. Core conductor theory and cable properties of neurons. *Comprehensive physiology*, pages 39–97, 1977.

[20] T.J. Sejnowski. Computational modeling of three-dimensional electrodiffusion in biological systems: application to the node of ranvier. *Biophysical journal*, 2008.

[21] T.J. Sejnowski and Ning Qian. An electro-diffusion model for computing membrane potentials and ionic concentrations in branching dendrites, spines and axons. *Biol. Cybern*, 62:1–15, 1989.

[22] D.I. Stephanova and H. Bostock. A distributed-parameter model of the myelinated human motor nerve fibre: temporal and spatial distributions of action potentials and ionic currents. *Biol. Cybern*, 73:275–280, 1995.

[23] David Sterratt, Bruce Graham, Andrew Gillies, and David Willshaw. *Principles of computational modelling in neuroscience*. Cambridge University Press, 2011.

[24] Ichiji Tasaki. The electro-saltatory transmission of the nerve impulse and the effect of narcosis upon the nerve fiber. *American Journal of Physiology-Legacy Content*, 127(2):211–227, 1939.

[25] JM Van Egeraat and JP Wikswo Jr. A model for axonal propagation incorporating both radial and axial ionic transport. *Biophysical journal*, 64(4):1287–1298, 1993.

[26] Thomas Andrew Waigh. *The physics of living processes: a mesoscopic approach*. John Wiley & Sons, 2014.

[27] Robert G. Young, Ann M. Castelfranco, and Daniel K. Hartline. The "lillie transition": Models of the onset of saltatory conduction in myelinating axons. *J Comput Neurosci*, 34:533–546, 2013.

9 Appendix: Discretization

9.1 The passive cable equation

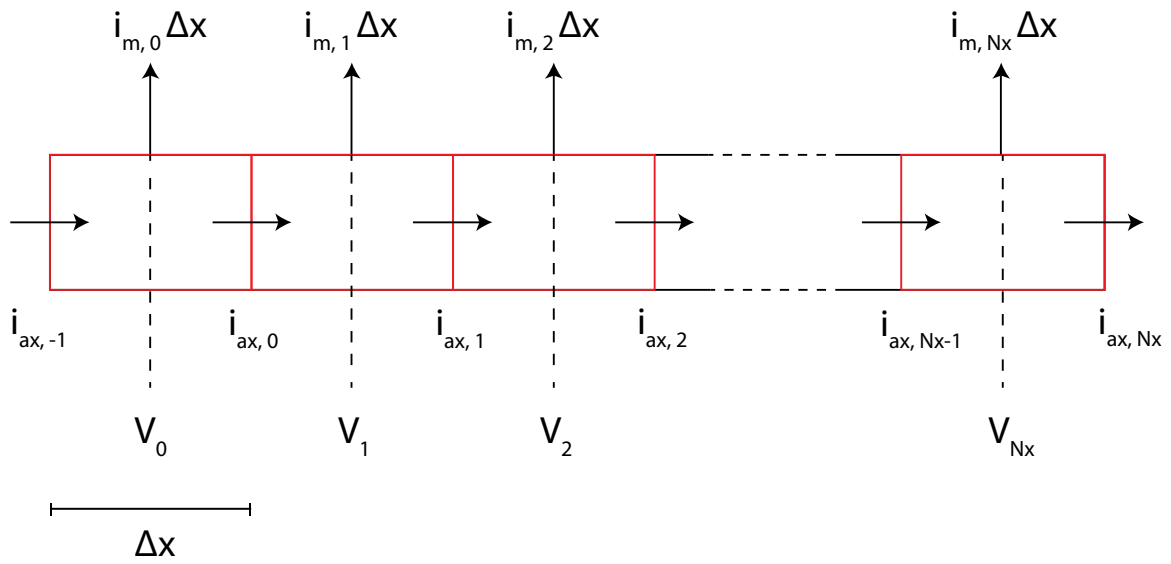

Figure 28: Discretization of an unmyelinated axon of total length L. The axon is split up into N_x segments of equal length $\Delta x = L/N_x$. Each segment has an associated membrane current and incoming/outgoing axonal currents.

In this section we discretize the passive cable equation (7) such that we can numerically solve it. Recall the form of the passive cable equation:

$$\tau \frac{\partial V(t,x)}{\partial t} = \lambda^2 \frac{\partial^2 V(t,x)}{\partial x^2} - V(t,x). \tag{53}$$

Consider x to be in the interval $[0, L]$. We split this interval up into N_x segments of equal length $\Delta x = L/N_x$ with $N_x + 1$ the amount of space lattice points. With this we can define $V_i(t) = V(t, i\Delta x)$ with $0 \leq i \leq N_x$ (see Fig. 28).
The derivative is given by the limit

$$\frac{\partial V(t,x)}{\partial x} = \lim_{h \to 0} \frac{V(t, x+h) - V(t,x)}{h}. \tag{54}$$

However, our space interval has been discretized and hence h has a smallest value given by Δx. This means that we can write the derivative as

$$\frac{\partial V(t,x)}{\partial x} \approx \frac{V(t, x+\Delta x) - V(t,x)}{\Delta x}. \tag{55}$$

This is the forward difference method as we consider V at a point $x + \Delta x$ to the right of x. Similarly we can define the backward and central differences respectively:

$$\frac{\partial V(t,x)}{\partial x} \approx \frac{V(t,x) - V(t, x-\Delta x)}{\Delta x}, \tag{56}$$

$$\frac{\partial V(t,x)}{\partial x} \approx \frac{V(t,x+\Delta x/2) - V(t,x-\Delta x/2)}{\Delta x}. \tag{57}$$

We will use the central difference method twice to approximate our second order spatial derivative

$$\frac{\partial^2 V(t,x)}{\partial x^2} = \frac{\frac{\partial V(t,x+\Delta x/2)}{\partial x} - \frac{\partial V(t,x-\Delta x/2)}{\partial x}}{\Delta x} = \frac{V(t,x+\Delta x) - 2V(t,x) + V(t,x-\Delta x)}{(\Delta x)^2}. \tag{58}$$

Substituting this expression into the cable equation and considering the point $x = i\Delta x$ gives us

$$\tau \frac{dV_i(t)}{dt} = \lambda^2 \frac{V_{i+1}(t) - 2V_i(t) + V_{i-1}(t)}{(\Delta x)^2} - V_i(t). \tag{59}$$

Having discretized the spatial dimension x, we now turn to the time t. Consider t to be on the interval $[0, T]$. We split this interval into N_t segments of equal length $\Delta t = T/N_t$ where we define the potential at the spatial point $x = i\Delta x$ and at time $k\Delta t$ to be $V_i^k = V(k\Delta t, i\Delta x)$ with $0 \leq k \leq N_t$.
Depending on which finite difference we consider for the time, we will arrive at the Forward or Backward Euler method.

9.1.1 (Explicit) Forward-Euler method

The simplest difference one could consider is the forward difference given by:

$$\frac{dV_i(t)}{dt} \approx \frac{V_i(t+\Delta t) - V_i(t)}{\Delta t}. \tag{60}$$

Substituting this expression into the cable equation and considering the time $k\Delta t$ for $k \geq 0$, we obtain the forward-Euler equation.

$$\tau \frac{V_i^{k+1} - V_i^k}{\Delta t} = \lambda^2 \frac{V_{i+1}^k - 2V_i^k + V_{i-1}^k}{(\Delta x)^2} - V_i^k. \tag{61}$$

Rewriting this equation gives us

$$V_i^{k+1} = \psi V_{i-1}^k + \phi V_i^k + \psi V_{i+1}^k, \tag{62}$$

where we define the dimensionless constants

$$\begin{aligned} \psi &= \frac{\Delta t}{\tau} \frac{\lambda^2}{\Delta x^2}, \\ \phi &= 1 - 2\psi - \frac{\Delta t}{\tau}. \end{aligned} \tag{63}$$

Hence we can see that the forward Euler method (62) is an explicit method since V^{k+1} at the next time step depends on the known values V^k at the previous time step. This makes this method very easy to implement, but it is known to suffer from numerical instability depending on the values one takes for $\Delta x, \Delta t$ [10]. For this reason, we instead choose to implement the backward-Euler method since this method does not suffer from the same numerical instabilities as the explicit method.

9.1.2 (Implicit) Backward-Euler method

For the backward-Euler method, we approximate the time derivative as follows:

$$\frac{\partial V_i(t)}{\partial t} \approx \frac{V_i(t) - V_i(t - \Delta t)}{\Delta t}. \tag{64}$$

Substituting this into the cable equation and considering the time $(k+1)\Delta t$ for $k \geq 0$, such that we avoid a negative time argument, we arrive at the backward-Euler equation.

$$\tau \frac{V_i^{k+1} - V_i^k}{\Delta t} = \lambda^2 \frac{V_{i+1}^{k+1} - 2V_i^{k+1} + V_{i-1}^{k+1}}{(\Delta x)^2} - V_i^{k+1}. \tag{65}$$

Using the dimensionless constants

$$\begin{aligned} \psi &= \frac{\Delta t}{\tau} \frac{\lambda^2}{\Delta x^2}, \\ \phi &= 1 + 2\psi + \frac{\Delta t}{\tau}, \end{aligned} \tag{66}$$

we can rewrite this equation to obtain

$$V_i^k = -\psi V_{i-1}^{k+1} + \phi V_i^{k+1} - \psi V_{i+1}^{k+1}. \tag{67}$$

From eq (67) we can see why this is an implicit method. At each time step one needs to solve a linear system of equations in order to compute the new potential values. Although this method is a bit harder to implement, it is superior to the explicit method since we do not have to worry about the numerical instabilities that can arise for certain choices of $\Delta t, \Delta x$.

9.1.3 Boundary conditions

Next we present possible boundary conditions. One type is the Dirichlet boundary condition for which we specify the values of V at the spatial end points.

$$\begin{aligned} V(t, 0) &= V_0, \\ V(t, L) &= V_L. \end{aligned} \tag{68}$$

These conditions at the end points are commonly denoted by "clamped-end" boundary conditions. We call the special case where V_0 or V_L equals the rest potential E_r, an "open-end" boundary condition. This can be easily seen by considering the definition of the potential $V = V_m - E_r$, $V_m = V_{ax} - V_o$. When $V = E_r$, then $V_m = 0$ which means that $V_{ax} = V_o$. Since the potential inside the axon equals the outside potential, this end is cut "open" which explains the name "open-end" boundary condition.
Another type is the Neumann boundary condition for which we specify the current at the end points.

$$\begin{aligned} \frac{\partial V(t, 0)}{\partial x} &= -i_{inj}(t) r_{ax}, \\ i_{inj}(t) &= \begin{cases} i_{inj} & t \leq t_{inj} \\ 0 & \text{else} \end{cases} \\ \frac{\partial V(t, L)}{\partial x} &= 0. \end{aligned} \tag{69}$$

Recall that in the derivation of the single cable equation we showed that $\partial V_{ax}(x,t)/\partial x$ is proportional to the longitudinal current $i_{ax}(x,t)$. Since $V = V_m - E_r = V_{ax} - V_o - V_r$, and V_o, V_r

are assumed spatially uniform, we have that $\partial V(x,t)/\partial x = \partial V_{ax}(x,t)/\partial x$. This shows that the two conditions above are indeed conditions for the longitudinal current inside the axon core. The first condition corresponds to injecting a current i_{inj} (see Fig. 28) at the beginning of the axon for a certain period of time while the second condition is called a "sealed-end" boundary since no current is allowed to exit through this end point.
In order to use the Neumann boundary conditions presented above in numerical simulations, we need to discretize them. Due to its simplicity, we choose to discretize them using forward differences:

$$\begin{aligned} \frac{\partial V^k(0)}{\partial x} &= \frac{V_0^k - V_{-1}^k}{\Delta x}, \\ \frac{\partial V^k(L)}{\partial x} &= \frac{V_{N_x+1}^k - V_{N_x}^k}{\Delta x}. \end{aligned} \tag{70}$$

Note that V_{-1}^k and V_{N_x+1} are potentials at non existing grid points. In order to use this method, we will then have to write V_{-1}^k and V_{N_x+1} in terms of V_0^k and V_{N_x} respectively by using the Neumann boundary conditions that we set. We can then replace V_{-1}^k and V_{N_x+1} with these expressions in the equations that we need to solve. For the Neumann boundary conditions (69), we obtain the relations:

$$\begin{aligned} V_{-1}^k &= V_0^k + i_{inj}^k r_{ax} \Delta x, \\ V_{N_x+1}^k &= V_{N_x}^k. \end{aligned} \tag{71}$$

9.1.4 Matrix form

Consider an axon subject to the Neumann boundary conditions (69). Using the implicit Euler method, the linear system of equations that we need to solve are:

$$\begin{aligned} V_0^k &= -\psi V_{-1}^{k+1} + \phi V_0^{k+1} - \psi V_1^{k+1}, \\ V_1^k &= -\psi V_0^{k+1} + \phi V_1^{k+1} - \psi V_2^{k+1}, \\ V_2^k &= -\psi V_1^{k+1} + \phi V_2^{k+1} - \psi V_3^{k+1}, \\ &\vdots \\ V_{N_x-1}^k &= -\psi V_{N_x-2}^{k+1} + \phi V_{N_x-1}^{k+1} - \psi V_{N_x}^{k+1}, \\ V_{N_x}^k &= -\psi V_{N_x-1}^{k+1} + \phi V_{N_x}^{k+1} - \psi V_{N_x+1}^{k+1}. \end{aligned} \tag{72}$$

For V_{-1}^k and V_{N_x+1} we substitute the equations (71) to obtain the linear system of equations:

$$\begin{aligned}
V_0^k + \psi i_{inj}^k r_{ax} \Delta x &= (\phi - \psi) V_0^{k+1} - \psi V_1^{k+1}, \\
V_1^k &= -\psi V_0^{k+1} + \phi V_1^{k+1} - \psi V_2^{k+1}, \\
V_2^k &= -\psi V_1^{k+1} + \phi V_2^{k+1} - \psi V_3^{k+1}, \\
&\vdots \\
V_{N_x-1}^k &= -\psi V_{N_x-2}^{k+1} + \phi V_{N_x-1}^{k+1} - \psi V_{N_x}^{k+1}, \\
V_{N_x}^k &= -\psi V_{N_x-1}^{k+1} + (\phi - \psi) V_{N_x}^{k+1}.
\end{aligned} \tag{73}$$

Which we can write in matrix form

$$\vec{V}^k = \boldsymbol{A} \vec{V}^{k+1}. \tag{74}$$

Where the components of the vectors and matrix are given by the linear system of equations above. Note that the matrix $\boldsymbol{A}$ is independent of the potential. Numerical simulations of the passive cable equation will then proceed as follows:

- We always start with an axon that is initially at rest. Meaning that $\vec{V}^0 = 0$.
- Next we calculate the matrix $\boldsymbol{A}$ by using the values of ψ and ϕ which we calculate from the relevant parameters.
- Afterwards we solve the matrix equation (74) to find the potential at the next time step $\vec{V}^1$.
- We then use the new potential to determine the next potential etc. We do this for all the time steps until we have determined the full time course of $\vec{V}$.

9.2 The active cable equation

In this section, we will discretize the Hodgkin & Huxley active cable equation and provide a procedure with which one can numerically solve the equations. Recall that the Hodgkin & Huxley equations are given by:

$$\frac{d}{4R_{ax}} \frac{\partial^2 V}{\partial x^2} = C_m \frac{\partial V}{\partial t} + \bar{g}_L (V - V_L) + \bar{g}_K n^4 (V - V_K) + \bar{g}_{Na} m^3 h (V - V_{Na}) \tag{75}$$

With the potassium and sodium rate variables given by the first order equations:

$$\begin{aligned}
\frac{dn}{dt} &= \alpha_n(V)(1 - n) - \beta_n(V) n, \\
\frac{dm}{dt} &= \alpha_m(V)(1 - m) - \beta_m(V) m, \\
\frac{dh}{dt} &= \alpha_h(V)(1 - h) - \beta_h(V) h.
\end{aligned} \tag{76}$$

Using the Implicit Euler method, we can discretize the Hodgkin & Huxley equation as follows:

$$C_m \frac{\partial V}{\partial t} = \frac{d}{4R_{ax}} \frac{\partial^2 V}{\partial x^2} - I_L - I_K - I_{Na},$$

$$\frac{C_m}{\Delta t}(V_i^{k+1} - V_i^k) = \frac{d}{4R_{ax}(\Delta x)^2}(V_{i-1}^{k+1} - 2V_i^{k+1} + V_{i+1}^{k+1}) - I_{L,i}^{k+1} - I_{K,i}^{k+1} - I_{Na,i}^{k+1},$$

$$V_i^k = V_i^{k+1} + \frac{d\Delta t}{4R_{ax}(\Delta x)^2 C_m}(-V_{i-1}^{k+1} + 2V_i^{k+1} - V_{i+1}^{k+1}) + \frac{\Delta t}{C_m}(I_{L,i}^{k+1} + I_{K,i}^{k+1} + I_{Na,i}^{k+1}),$$

$$V_i^k = V_i^{k+1} + \Psi(-V_{i-1}^{k+1} + 2V_i^{k+1} - V_{i+1}^{k+1}) + \frac{\Delta t}{C_m}(I_{L,i}^{k+1} + I_{K,i}^{k+1} + I_{Na,i}^{k+1}),$$

$$V_i^k = -\Psi V_{i-1}^{k+1} + (1 + 2\Psi)V_i^{k+1} - \Psi V_{i+1}^{k+1} + \frac{\Delta t}{C_m}(I_{L,i}^{k+1} + I_{K,i}^{k+1} + I_{Na,i}^{k+1}),$$

$$V_i^k = -\Psi V_{i-1}^{k+1} + (1 + 2\Psi)V_i^{k+1} - \Psi V_{i+1}^{k+1} + \frac{\Delta t}{C_m}\Big[\bar{g}_L(V_i^{k+1} - V_L),$$

$$+ \bar{g}_K(n_i^{k+1})^4(V_i^{k+1} - V_K) + \bar{g}_{Na}(m_i^{k+1})^3 h_i^{k+1}(V_i^{k+1} - V_{Na})\Big],$$

$$\boldsymbol{V_i^k + \omega_i^{k+1} = -\Psi V_{i-1}^{k+1} + (1 + 2\Psi + \phi_i^{k+1})V_i^{k+1} - \Psi V_{i+1}^{k+1}},$$

$$\Psi = \frac{d\Delta t}{4R_{ax}(\Delta x)^2 C_m},$$

$$\phi_i^{k+1} = \frac{\Delta t}{C_m}\Big[\bar{g}_L + \bar{g}_K(n_i^{k+1})^4 + \bar{g}_{Na}(m_i^{k+1})^3 h_i^{k+1}\Big],$$

$$\omega_i^{k+1} = \frac{\Delta t}{C_m}\Big[\bar{g}_L V_L + \bar{g}_K(n_i^{k+1})^4 V_K + \bar{g}_{Na}(m_i^{k+1})^3 h_i^{k+1} V_{Na}\Big]. \tag{77}$$

For the boundary conditions, we use the same method described in our discretization of the passive cable model. Again we can write the set of equations above in terms of the matrix equation:

$$\vec{V}^k + \vec{\omega} = \boldsymbol{A}\vec{V}^{k+1}. \tag{78}$$

Where $\vec{\omega}$ consists of the elements ω_i^{k+1} and the matrix $\boldsymbol{A}$ depends on Ψ and ϕ_i^{k+1}.
In order to solve the matrix equation above, we need to know the values of the rate variables at time $k+1$. We know that the dimensionless variables are given by the differential equations:

$$\frac{dy}{dt} = \alpha_y(1 - y) - \beta_y y \quad \text{for} \quad y = n, m, h. \tag{79}$$

Discretizing this differential equation by using the backward difference gives us

$$\begin{aligned} \frac{y_i^{k+1} - y_i^k}{\Delta t} &= \alpha_{y,i}^{k+1}(1 - y_i^{k+1}) - \beta_{y,i}^{k+1} y_i^{k+1}, \\ y_i^{k+1} &= \frac{y_i^k + \Delta t \alpha_{y,i}^{k+1}}{1 + \Delta t \alpha_{y,i}^{k+1} + \Delta t \beta_{y,i}^{k+1}}. \end{aligned} \tag{80}$$

We see that in order to determine the rate variables at time $k+1$, we need to know the potential at time $k+1$. Since $\alpha_{y,i}^{k+1}$ and $\beta_{y,i}^{k+1}$ both depend on V_i^{k+1}. This makes the problem much more complex so in order to make the computations tractable we decided to simplify the problem by setting:

$$y_i^{k+1} = \frac{y_i^k + \Delta t \alpha_{y,i}^k}{1 + \Delta t \alpha_{y,i}^k + \Delta t \beta_{y,i}^k}. \tag{81}$$

We argue that by taking the time step Δt small enough, the error caused by this simplification is acceptable. We will see from the results that we obtain that this is indeed the case. Hence, given an initial condition for the rate variables and potential, we can calculate the values of the rate variables at time $k+1$. We choose our initial conditions for the rate varables to be:

$$\frac{dy}{dt}(t = 0, x) = 0 \quad \text{for} \quad y = n, m, h. \tag{82}$$

Which, when plugged into eq (76), yields us the initial condition for the rate variables:

$$y_i^0 = \frac{\alpha_{y,i}^0}{\alpha_{y,i}^0 + \beta_{y,i}^0}. \tag{83}$$

Now we have everything we need in order to solve the Hodgkin & Huxley equations. Below is the numerical procedure we used.

- One start with an axon that is initially at rest everywhere, meaning $V_i^0 = 0$ for all spatial points i.
- Next we calculate the values of the rate variables y_i^0 at time $t = 0$ by plugging the values for V_i^0 into the voltage dependent expressions for the rate coefficients $\alpha_{y,i}^0, \beta_{y,i}^0$ in eq (83).
- By using the backward difference on eq (82), we have that $y_i^1 = y_i^0$. This allows us to start the iterative procedure.
- Using the values of y_i^1, we then determine the values of ϕ_i^1 and ω_i^1 from eq (77).
- Next, we calculate the matrix $\boldsymbol{A}$ by using the values of ϕ_i^1 and Ψ, and we add the values of ω_i^1 to V_i^0. With this, we are ready to solve for V_i^1 by solving the matrix equation (78).
- After having calculated V_i^1, we determine y_i^2 by using eq (81).
- Then, by using y_i^2, we redo the steps above to determine V_i^2. Doing this for all time steps yields us V as a function of time and space.